Hypoxia and HIF-1 trigger Marek's Disease Virus reactivation in lymphoma-derived latently infected T lymphocytes

Corentin Mallet, Jade Cochard, Sébastien Leclercq, Laëtitia Trapp-Fragnet, Philippe Chouteau, Caroline Denesvre

RESEARCH ARTICLE

Hypoxia and HIF-1 trigger Marek's Disease Virus reactivation in lymphomas-derived latently-infected T lymphocytes

Corentin Mallet[1], Jade Cochard[2], Sébastien Leclercq[1], Laetitia Trapp-Fragnet[1], Philippe Chouteau[2], Caroline Denesvre[1]*

[1] ISP, INRAE, Université de Tours, 37380 Nouzilly, France

[2] INSERM U1259, Université de Tours and CHRU de Tours, France.

* Corresponding author : Mailing address : Laboratoire de Biologie des Virus Aviaires, INRAE-Université de Tours, UMR1282 ISP, Centre INRAE Val de Loire, 37380 Nouzilly, France.

Phone : (+33) 2 47 42 76 19

E-mail: caroline.denesvre@inrae.fr

Running head : Hypoxia triggers MDV reactivation

Abstract : 249 words; Importance: 149 words; 10 figures, 3 tables

ABSTRACT

Latency is a hallmark of herpesviruses, allowing them to persist into their host without virions production. Acute exposure to hypoxia (below 3% O_2) was identified as a trigger of latent-to-lytic switch (reactivation) for human oncogenic gamma-herpesviruses (KSHV and EBV). Therefore, we hypothesized that hypoxia could also induce reactivation of Marek's disease virus (MDV), sharing biological properties with EBV and KSHV (notably oncogenic properties), into lymphocytes. Acute exposure to hypoxia (1% O_2) of two MDV-latently infected cell lines derived from MD tumors (3867K and MSB-1) induced MDV reactivation. A bioinformatic analysis of the RB-1B MDV genome revealed 214 putative hypoxia-response element consensus sequences on 119 open reading frames. RT-qPCR analysis showed five MDV genes strongly upregulated early after hypoxia. In 3867K cells under normoxia, pharmacological agents mimicking hypoxia (MLN4924 and $CoCl_2$) increased MDV reactivation, but to a lower level than real hypoxia. Overexpression of wild-type or stabilized human hypoxia inducible factor-1α (HIF-1α) in MSB-1 cells in normoxia also promoted MDV reactivation. In such conditions, lytic cycle was detected in cells with a sustainable HIF-1α expression, but also in HIF-1α negative cells, indicating that MDV reactivation is mediated by HIF-1, in a direct and/or indirect manner. Lastly, we demonstrated by a reporter assay that HIF-1α overexpression induced the transactivation of two viral promoters, shown upregulated in hypoxia. These results suggest that hypoxia may play a crucial role in the late lytic replication phase observed *in vivo* in MDV-infected chickens exhibiting tumors, since a hypoxic microenvironment is a hallmark of most solid tumors.

IMPORTANCE

Latent-to-lytic switch of herpesviruses (aka reactivation) is responsible for pathology recurrences and/or viral shedding. Studying physiological triggers of reactivation is therefore important for health to limit lesions and viral transmission. Marek's disease virus (MDV) is a potent oncogenic alpha-herpesvirus establishing latency in T-lymphocytes and causing lethal T-lymphomas in chickens. *In vivo*, a second lytic phase is observed during tumoral stage. Hypoxia being a hallmark of tumors, we wondered whether hypoxia induces MDV reactivation in latently-infected T-lymphocytes, like previously shown for EBV and KSHV in B-lymphocytes. In this study, we demonstrated that acute hypoxia (1% O2) triggers MDV reactivation in two MDV transformed T-cell lines. We provide some molecular basis of this reactivation by showing that hypoxia inducible factor (HIF-1) overexpression induces MDV reactivation to a similar extend than hypoxia after 24 hours. Hypoxia is therefore a reactivation stimulus shared by mammalian and avian oncogenic herpesviruses of different genus.

KEYWORDS: Marek’s disease virus, reactivation, hypoxia, lymphocytes, HIF-1.

Herpesviruses are large DNA viruses causing various types of pathologies, in clinical signs and severity, including recurrent local infections and cancers. Such pathologies are associated with the persistence of the virus in the host after infection and its biphasic life cycle, either latent or lytic. The latent cycle consists of a state in which the viral genome persists into the host cell nucleus, with no infectious virions production and a limited number of viral products (either RNA and/or proteins), avoiding detection by the immune system [1]. In contrast, the lytic cycle leads to virions production, cell death, and virus shedding. Each virus species establishes latency in a unique cell type and in a limited number of cells. The identification of the factors and molecular mechanisms governing the switch from latent-to-lytic cycle, named reactivation, is of major importance to limit the recurrence of lesions and viral shedding. Various environmental factors have been identified as triggering reactivation: fever or UV light for herpes simplex virus (HSV-1, aka human herpesvirus 1) [2], and immune system aging for human cytomegalovirus (CMV, aka human herpesvirus type 5) and Epstein-Barr virus (EBV, aka human herpesvirus type 4) [3]. Recently, low oxygen level or hypoxia (≤ 3%) was identified as a potent reactivation factor for gamma-herpesviruses. Initially demonstrated for the Kaposi sarcoma-associated virus (KSHV, aka human herpesvirus type 8) in B cells [4], hypoxia was also shown to induce the reactivation of two other gamma-herpesviruses in B-cells, EBV and the murine herpesvirus type 4 (MHV-4) [5, 6]. For these three viruses, the hypoxia inducible factor 1 (HIF-1) was shown as a molecular determinant triggering reactivation, by turning-on the expression of at least one critical gene in the initiation of the lytic cycle: BZLF-1 for EBV [5, 7], ORF50-rta for KSHV [8, 9] and MHV-4 [6]. HIF-1 is a transcription factor whose activity is tightly regulated by oxygen [10]. HIF-1 is a heterodimer constituted of two sub-units, HIF-1α and HIF-1β, found in the entire animal kingdom [11]. HIF-1 protein regulation is based on HIF-1α degradation or stabilization,

depending on the percentage of oxygen. In normal oxygen conditions (normoxia; 21%, v/v), HIF-1α is quickly degraded by the proteasome after hydroxylation of three amino acids (Pro402, Pro564, Asn803), Von Hippel Lindau (VHL) binding, and ubiquitinylation (reviewed in [10, 12]). In normoxia, HIF-1α half-life is below 5 minutes [13]. In hypoxia, the prolyl-4-hydroxylases modifying HIF-1α are non-functional [14] and HIF-1α is stabilized [15]. Stabilized HIF-1α is subsequently translocated into the nucleus, where it dimerizes with the constitutively expressed HIF-1β subunit leading to an active HIF-1. The HIF-1 heterodimer then binds to hypoxia response element sequences (HREs) located within the promoter of target genes, leading to their transcription. HIF-1 target genes are involved in metabolism (lipids, carbohydrates), angiogenesis, erythropoiesis, and their expression allows an adaption to low oxygen conditions at cell, tissue, or organism level [10].

Marek's disease virus (MDV, aka Gallid herpesvirus type 2), is an alpha-herpesvirus from the Mardivirus genus that causes immunosuppression and lethal T- lymphomas in chickens. After entry through the respiratory tract, MDV infects B- and T-lymphocytes causing an early cytolytic infection, between 3 and 7 days post-infection (dpi) [16, 17]. At about 7 dpi, MDV establishes latency in a subset of T-lymphocytes, mostly CD4-positive [18], and its genome integrates into the host's genome telomeres [19-21]. During latent infection, a few MDV products are expressed: the Meq oncoprotein [22], several non-coding latency associated transcripts (LATs) [23, 24] as well as several micro RNAs (miRNAs) [25, 26]. Latent infection in T-cell is considered necessary for MDV transformation, which occurs 3 to 4 weeks post-infection. According to Calnek's model [18], a second lytic cycle called 'late cytolytic infection' occurs in lymphoid organs at a later time post-infection, when tumorigenesis is already established. MD tumors have been shown to contain 0.1% of CD4+ T-cells in lytic cycle [27], probably due to the reactivation of MDV. The stimuli triggering MDV reactivation

in lymphoid organs and tumors *in vivo* are still poorly known [28]. Hypoxia has been depicted as a common feature in solid tumors' microenvironment [29], notably when tumors cells rapidly proliferate, resulting in poor oxygen supply in the center of the tumor due to a lack of vascularization [30, 31]. Although hypoxia has not been demonstrated in Marek's disease (MD) T-lymphomas yet, we assumed that hypoxia exists in MD tumors due to their extremely rapid growth in chickens. By analogy with what has been reported for gamma-herpesviruses, we wondered whether hypoxia may contribute to MDV reactivation in MD lymphomas. In this study, our aim was to explore whether hypoxia can induce MDV reactivation in latently-infected T-cells. To this end, we used two well characterized cell lines established from MD lymphomas, MSB-1 [32, 33] and 3867K [34]. We show for the first time that hypoxia (1% O_2) induces MDV reactivation in T-cell lines *in vitro*. Using overexpression of HIF-1α in normoxia, we show that this transcription factor plays a crucial role in MDV reactivation. Altogether these findings provide new insights on MDV reactivation mechanisms.

RESULTS

Hypoxia increases the proportion of 3867K cells in lytic cycle.

To determine whether hypoxia can induce MDV reactivation, we used a T- lymphoid cell line latently-infected with the very virulent recombinant RB-1B 47eGFP, the 3867K cell line [34]. When virus reactivates, the lytic pUL47eGFP tegument protein is expressed, allowing the detection of GFP-positive cells [34, 35]. To start, 3867K cells were cultivated either in normoxia (at 21% O_2) or in hypoxia (at 1% O_2) for 72 hours (h). Viral reactivation was measured by flow cytometry by determining the percentage of GFP-positive cells in live cells. Under normoxic condition, the live GFP-positive cells represented 0.85% of the total cells

(Fig. 1A, left panel), corresponding to spontaneous reactivation. In hypoxia, live GFP-positive cells increased to 4%, i.e. 4.7-fold compared to normoxic conditions (Figure 1A, right panel). In both conditions, EGP-positive cells mean fluorescence was relatively low (about 70 in arbitrary units) (vs 5 to 10 arbitrary units in latently-infected cells), consistent with the low expression of pUL47eGFP during the lytic cycle in lymphocytes. In addition, the cellular mortality increased upon hypoxia (eFluor 780-positive cells), with dead cells representing 51.8 % of the total cells in hypoxia compared to 12.5% in normoxia (Figure 1A).

To confirm that the expression of pUL47eGFP reflected the switch to lytic cycle and not just a transcriptional activation of *UL47eGFP* expression under hypoxia, we verified by fluorescence microscopy the expression of two other late viral proteins essential for MDV infectivity: the major tegument protein VP22 and glycoprotein B (gB). Both VP22 and gB were expressed in nucleated GFP-positive cells, with similar localization in normoxia and hypoxia, consistent with the fact that pUL47eGFP-positive cells underwent a lytic cycle in both conditions (Figure 1B). In hypoxia, we noticed numerous cells emitting a low green fluorescence signal devoid of nucleus (Hoechst-negative), cells which were not stained for VP22 or gB (Figure 1B). Such cells were absent when viable cells (efluor 780-negative) were cell-sorted by flow cytometry before VP22 antibody staining (Figure 1C and below). Therefore, these enucleated green cells correspond most likely to a subpopulation of dead cells with an increased autofluorescence intensity and not to viral reactivation prior to cell death.

We next determined whether MDV reactivation was time-dependent under hypoxia. To this end, 3867K cells were cultivated in normoxia or hypoxia for 96 h and the percentage of reactivation was estimated every 24 h through pUL47eGFP expression by flow cytometry. While the percentage of live GFP-positive cells among live cells remained low in normoxia at

every time points (≤2%), it increased progressively approximatively 4-fold in hypoxia, from 2.5% to 9.5% between 24 and 96 h (Figure 1D). Cell mortality was between 12% and 25% in normoxia and between 32% and 66% in hypoxia (Table 1).

To further confirm that cells reactivating MDV under hypoxia are fully MDV productive, we determined the number of MDV genome copies per cell by quantitative PCR (qPCR) under normoxic and hypoxic conditions during 96 h (Figure 1E). In normoxia, the MDV genome copy number was below 5 x 10^7 per 10^6 cells at all time points tested, corresponding mostly to viral genomes integrated into the host genome. In hypoxia, MDV genome copy number per 10^6 cells increased progressively approximatively 4-fold. Such increase demonstrates that MDV reactivation in hypoxic cells is associated with an increased production of MDV genomes in these cells.

Hypoxia increases viral lytic genes expression in 3867K T-cell line, notably *ICP4*, *ICP27*, *UL39*, *UL41* and *UL49.*

In order to study the effect of hypoxia on viral genes expression, we next performed a bio-informatic analysis on the complete RB-1B genome to locate and enumerate all putative HREs in the promoter area of each identified open reading frame (ORF) (incl. hypothetical ones). In total, we identified 214 putative HREs on 119 ORFs (140 ORFs having been estimated on this genome [36]). The number of predicted HREs per promoter varied from 1 to 5, at the most. Note that *UL47*, *UL49* encoding VP22, and *UL27* encoding gB showed 1, 3, and no HRE respectively. Among MDV genes we selected sixteen lytic genes, thirteen with putative HREs and three without (Figure 2A): two immediate early (IE) genes (*ICP4* and *ICP27*), five early (E) genes (including *UL39* encoding the ribonucleotide reductase large sub-unit (RR1) and *UL41* encoding the viral host shutoff protein (VHS)) and nine late (L) genes

178 (including *UL47*, *UL49*, and *UL27*). *UL13*, *UL27*, and *UL48* are devoid of HRE in the promoter
179 area analyzed.
180 We assessed the effect of hypoxia on the expression of these sixteen viral transcripts
181 encoding lytic proteins by reverse transcriptase qPCR (RT-qPCR) over a 72-h period. The
182 expression of *Meq*, which is expressed in both latent and lytic phases was also quantified. Of
183 these seventeen genes, eleven (including UL47) were slightly upregulated (3- to 7-fold) 24 h
184 after hypoxia compared to normoxia, while five were greatly upregulated: the two IE genes,
185 *ICP4* and *ICP27* were upregulated 18- and 16-fold, respectively; two E genes, *UL39* and *UL41*
186 were upregulated 28- and 12-fold, respectively; and one L gene, *UL49*, was upregulated 17-
187 fold (Figure 2B). The high expression of *UL49* at that time point was striking. At 48 h of
188 hypoxia, all sixteen lytic genes (IE, E, and L) showed a mRNA expression at least 10-fold
189 higher (between 11- and 31-fold) than in normoxic conditions. At 72 h of hypoxia, the
190 expression of all lytic genes was still high, between 11- and 60-fold that of normoxia. At that
191 time, *ICP4*, ICP27, *UL39*, *UL41*, and *UL49* were still the most upregulated genes (> 40-fold),
192 like at 24 h. At 48 and 72h of hypoxia, *US7* encoding gI was also found highly upregulated.
193 The six most upregulated genes contain at least one HRE upstream (-) or downstream (+) of
194 their starting codon, which are strictly conserved in Md5 genome, another very virulent
195 MDV strain: *ICP4* (+49), *ICP27* (-165), *UL39* (-396, -654), *UL41* (-106, -356), *UL49* (-136, -285, -
196 301), and *US7* (-15, -90, -105). Note that *meq* expression was increased but less than all lytic
197 genes at 48 and 72h. All together, these results show that hypoxia induced the expression of
198 all viral lytic genes assessed, with a few genes upregulated, most likely via HRE.
199
200 ***MDV reactivation induced by hypoxia is not restricted to a cell line or a MDV genotype.***

To investigate whether hypoxia-induced reactivation is restricted to the 3867K cell line and/or to the RB-1B virus, we examined the effect of hypoxia on the most frequently used MD derived-cell line (MSB-1) obtained with the virulent BC-1 MDV strain, and whose reactivation is not traceable with a fluorescent gene. Therefore, to monitor MDV reactivation, we first quantified MDV genome copy numbers under normoxic and hypoxic conditions over a 96-h period (Figure 3A). The number of MDV genome copies per million cells was below 5×10^7 at all time points under normoxia. It increased from 4.6×10^7 at 24 h to 2.7×10^8 at 96 h under hypoxia. The fold-changes between hypoxia and normoxia increased over time, except for an inflection point at 72 h (which is probably due to a high mortality recorded in hypoxia starting at 48 h) (Table 1). This tumoral cell line also exhibited a high rate of mortality, even in normoxic condition (between 25% and 44%) (Table 1). Reactivation was next verified by examining the expression of VP22 after antibody staining by fluorescence microscopy (Figure 3B). A strong VP22 signal was visible in the cytoplasm of cells, much more frequently in hypoxia than in normoxia at 24 and 48 h. Numerous apoptotic nuclei were visible in normoxia and hypoxia, in accordance with the high mortality (as reported above). By counting VP22-positive cells among all cells exhibiting non-apoptotic nucleus by fluorescence microscopy, we estimated the % of MSB-1 reactivation at 3.2% and 7.3% after 24 h and 48 h of hypoxia, respectively, compared to < 1% in normoxia at both time points.

To confirm that viral reactivation was indeed induced by hypoxia in MSB-1, we quantified mRNA expression of sixteen lytic genes as well as *meq* by RT-qPCR as performed earlier for 3867K. The fold-changes between hypoxic and normoxic conditions are shown in Figure 3C. At 24 h of hypoxia, only *UL39* and *UL49* were upregulated > 10-fold compared to normoxia, while the other genes were upregulated 2- to 5-fold. At 48 h of hypoxia, all genes were

225 expressed > 10-fold (between 14 and 74-fold), with *ICP4*, *UL39*, *UL41*, *UL49*, and *US7* being
226 the most upregulated (≥ 35-fold). This was similar to that observed in 3867K cells except that
227 the fold-changes were globally higher at that time point (48 h) in MSB-1 than in 3867K. At 72
228 h of hypoxia, a gene expression for all genes was lower than at 48 h, as observed for DNA
229 genome copies.
230 Therefore, acute hypoxia induced MDV reactivation in both MSB-1 and 3867K cell lines alike,
231 although MSB-1 cells showed a higher viral gene expression and mortality compared to
232 3867K.
233
234 ***Hypoxia induces MDV reactivation in HIF-1α-positive cells and activates the expression of***
235 ***HIF-1 cellular target genes.***
236 Among HIFs, HIF-1α is the major cell regulator in hypoxia and the most ubiquitous. HIF-1α
237 has been shown to trigger viral reactivation in hypoxic conditions in three gamma-
238 herpesvirus [4-6]. To investigate the role of HIF-1α in MDV reactivation during hypoxia, we
239 first studied the expression of HIF-1α in 3867K and MSB-1 grown under hypoxia compared
240 to normoxia by fluorescence microscopy. To this end, both cell lines were grown in both
241 conditions for 48 h and live cells were sorted by flow cytometry before staining. The chicken
242 HIF-1α protein was detected by immunofluorescence, whereas virus reactivation was
243 detected with pUL47eGFP expression for the 3867K cell line and after VP22 immunostaining
244 for MSB-1 cells. Note that in these conditions, all 3867K cells emitting green fluorescence
245 have a nucleus (Figure 4). In normoxia, HIF-1α was almost undetectable in both 3867K and
246 MSB-1, indicating that HIF-1α was not stabilized in these transformed T-cells (Figure 4A-B,
247 upper panels). In contrast, in hypoxia, almost all 3867K and MSB-1 cells were HIF-1α-positive
248 as expected when this protein is stabilized (Figure 4A-B, lower panels). The quantification of

the HIF-1α signal per cell confirmed that the fluorescence intensity was significantly higher in hypoxia than in normoxia in both cell lines, although weak notably in 3867K (Figure 4 C-D). These results indicated that HIF-1α was indeed stabilized in both cell lines cultivated under hypoxia. In hypoxia, among HIF-1α-positive cells, only a fraction of the live cells was expressing lytic viral proteins as earlier.

To verify that HIF-1α stabilization under hypoxia was functional in MDV T-cell lines, we examined HIF-1 transcriptional activity by measuring the expression of three HIF-1 cellular target genes identified for mammals [10]: *GLUT1*, the glucose transporter 1; *LDHA*, the pyruvate dehydrogenase A which mediates the conversion of pyruvate in lactate; and *iNOS*, the inducible nitric oxide synthetase. Cells (3867K and MSB-1) were cultivated under hypoxia or normoxia for 72 or 96 h and the mRNA levels of *GLUT1*, *LDAH*, and *iNOS* were measured by RT-qPCR every 24 h. In 3867K cells, all three genes were upregulated under hypoxia compared to normoxia at all time points (Figure 5A). Most fold-changes ranged between 5 and 15. We also verified in the same manner, that HIF-1 was functional in MSB-1 cells cultivated in hypoxia (Figure 5B). Taken together, we demonstrated that HIF-1α was stabilized under hypoxia exposure in both 3867K and MSB-1 cell lines and that HIF-1 was functional.

Hypoxia-mimicking pharmacological agents $CoCl_2$ and MLN4924 induce MDV reactivation in 3867K cells.

To study the specific role of HIF-1α stabilization in MDV reactivation, we tested two pharmacological agents, MLN4924 and $CoCl_2$, known to stabilize HIF-1α in mammalian cells in normoxia by reducing its degradation. 3867K cells were cultivated in the presence of each drug at different concentrations for 24 h in normoxia (two independent experiments). MDV

reactivation and cell mortality were assessed by flow cytometry as described earlier. Both drugs increased MDV reactivation in a dose-dependent manner compared to mock-treated cells as negative control (Figure 6A). The mortality observed with MLN4924 and $CoCl_2$ at the upper doses was 22.85% and 14.1%, respectively. Cells were treated with sodium butyrate (0.5 mM for 48 h), an inhibitor of histone deacetylases, as positive control of reactivation, leading to a 5.3-fold increase of reactivated live cells (with a mortality of 18.6% of total cells). $CoCl_2$ treatment (250 µM) led to a 2.3-fold increase of reactivated live cells compared to control. MLN4924 treatment at 1 and 2.5 µM induced a greater reactivation, with 3.7- and 4.2-fold increase, respectively. MLN4924's effect was time-dependent since no reactivation was observed with 1 µM after 8 h of treatment compare to control. MDV reactivation being milder with $CoCl_2$ than with MLN4924 treatment, subsequent analyses were only performed with MLN4924. We next examined HIF-1α and MDV lytic antigens expression by fluorescence microscopy on 3867K cells treated with 1 µM MLN4924 for 24 h. HIF-1α was detected in most MLN4924-treated cells including reactivating MDV cells but not in DMSO-treated cells (control) (Figure 6B). To confirm reactivation, the RNA expression of four lytic genes (*ICP4*, *UL39*, *UL49*, and *UL13*) was measured by RT-qPCR and compared to DMSO-treated cells. The expression of all four viral genes increased as expected in two independent experiments (Figure 6C). Next, we examined the activity of HIF-1 by measuring the mRNA expression of two cellular HIF-1 targets (*LDAH* and *GLUT-1)*. Surprisingly the expression of these two genes did not change compared to the DMSO control. All together, these results showed that MLN4927 induces MDV reactivation in 3867K cells, but the role of HIF-1α stabilization in that process could not be clearly demonstrated. The way by which MLN4924 may induce MDV reactivation herein is discussed later.

Human HIF-1α is functional in chicken cells.

To further clarify the role of HIF-1α in MDV reactivation and in absence of validated chicken HIF-1α tools, we verified the functionality of the human HIF-1α (hHIF-1α) in chicken cells after transient transfection with expressing vectors. Lymphocytes are cells known to be extremely difficult to transfect with plasmids. Therefore, we first optimized the transfection efficiency by using the Neon® nucleofector technology, a technology which allows high transfection efficiency with human lymphocytes. An orange fluorescent reporter plasmid (pPB tdTomato) of large size (8.67kb) was used for that purpose. At 24 h post-transfection, transfection efficacy was 6.7% in 3867K cells and 24.7% in MSB-1 cells, based on Tomato-fluorescence using flow cytometry.

We next studied the functionality of hHIF-1α in MSB-1 cells, which gave the higher rate of transfection. To this end, we used two hHIF-1α: the hHIF-1α WT or a stabilized mutant (hHIF-1α mut). This mutant has three amino-acids mutated to prevent its hydroxylation and subsequent degradation in the presence of a high-rate of oxygen (*ie,* 21%). It is therefore stabilized in normoxia in contrast to the WT which is degraded by the proteasome. Using Neon® technology, MSB-1 cells were transfected with the pHRE-d2EGFP reporter plasmid and a vector expressing hHIF-1α (mut or WT). When HIF-1α is expressed at a sufficient level, the eGFP reporter gene is expressed. The pHRE-d2EGFP plasmid encodes a destabilized eGFP, with a short half-life of 2 h, under the control of a minimal promoter containing 5 HRE sequences. Due to its destabilization, the eGFP visualized in cells is therefore the result of recently synthetized proteins and not the result of accumulated proteins overtime. The eGFP expression was monitored by fluorescence microscopy at 8, 24, and 48 h post-transfection (Figure 7). In hHIF-1α mut-expressing cells, the percentage of GFP-positive cells was at the highest (28.5 %) at 24 h post-transfection (Figure 7A). Note that this percentage is consistent

with the % of transfection that we measured with the pPB tdTomato. The % of GFP-positive cells decreased at 48 h (13.1%), probably due to the resuming of cell division and the increase of non-transfected cells. In the absence of hHIF-1α mut (pHRE-d2EGFP only), the percentage of GFP-positive cells was < 4.2% at all time points. These data indicate that hHIF-1α mut transactivates a minimal promoter harboring (5 x) HRE in MSB-1. With the hHIF-1 WT, the percentage of GFP-positive cells was of 7.1% at 24 h post-transfection (Figure 7B), which is much less than with hHIFα mut as expected. This indicates that, when overexpressed, hHIF-1α WT is also capable of transactivating a promoter with HREs, but to a lesser extent than the hHIF-1α mut. Altogether, these data show that the human HIF-1α (WT or stabilized) is functional in chicken T-cells, indicating that it can dimerize with the avian HIF-1ß. Additionally, we demonstrated for the first time that the Neon technology provides good transfection rates in an avian lymphoid cell line.

HIF-1α overexpression triggers MDV reactivation in MSB-1 cells.

To determine whether HIF-1α could play a role in MDV reactivation, hHIF-1α (mut or WT) was overexpressed in MSB-1 cells cultured in normoxia. To this end, MSB-1 cells were transfected with either expression vector and were examined 24 h post-transfection by fluorescence microscopy after immunostaining for HIF-1α and MDV lytic antigens. The percentage of HIF-1α-positive cells was 13% and 3.8% with hHIF-1α mut and WT, respectively (Figure 8A). This suggested a “mild” stabilization of HIF-1α in the cells transfected with hHIF-1α WT and a greater stabilization in the cells transfected with hHIF-1α mut, as previously observed in Fig. 7. Note that the detection of HIF-1α by immunofluorescence is less sensitive of 13 to 21% at detecting HIF-1α expression than with the reporter gene assay. Therefore, the percentage of HIF-1α-positive cells may be slightly

345 underestimated herein. The percentage of MDV reactivation was then evaluated by counting
346 the relative number of ICP4/VP22-positive cells. The percentage of reactivated cells was
347 about 3% with both hHIF-1α WT and mut and < 1% with the empty pcDNA3 (0.5%) and non-
348 transfected cells (0.7%) (Figure 8B). This indicates that not all cells expressing HIF-1α
349 reactivated, as observed earlier in hypoxic condition.
350 We next examined whether MDV reactivation occurs only in cells in which HIF-1α is
351 detectable. To this end, the percentage of cells expressing both HIF-1α and MDV antigens
352 (VP22/ICP4) were counted by fluorescence microscopy (Figure 8C and D). The % of double-
353 labelled cells was 0.9% with HIF-1α mut and of 0.2% with HIF-1α WT (Figure 8C). Therefore
354 surprisingly > 2% of reactivated cells were *not* HIF-1α-positive. These results demonstrate
355 that HIF-1α mutant and WT expression triggers MDV reactivation. They also suggest a direct
356 and/or indirect effect of HIF-1α on MDV reactivation, discussed below.
357
358 ***HIF-1α over-expression activates MDV UL39 and UL49 viral promoters.***
359 To further explore the molecular mechanism by which hypoxia induces MDV reactivation,
360 we examined if the stabilized hHIF-1α can transactivate the promoters of the five MDV lytic
361 genes, that we found upregulated in hypoxia (ICP4, ICP27, UL39, UL41 and UL49) (Figure 2A).
362 For that, we cloned the five HRE-containing promoter regions of these genes upstream of a
363 destabilized firefly luciferase (fLuc), as well as two MDV promoters (UL36, UL45) devoid of
364 HRE as controls. The promoter constructs were transfected in ESCDL-1 chicken cells in
365 normoxia, with or without the stabilized hHIF-1α vector. A Renilla Luciferase plasmid (pRL)
366 was also co-transfected to standardize the transfection efficiency. At 24 h post-transfection,
367 the expression of the stabilized hHIF-1α was verified (Figure 9A) and the relative luciferase
368 activity (ratio of the fLuc/RL) was calculated (Figure 9B). In absence of the stabilized hHIF-1α,

369 the basal activity of each promoter was low (relative luciferase activity <0.5). The ectopic
370 expression of the stabilized hHIF-1α induced a significant increase of the transcriptional
371 activity for all promoters. Despite this increase, the promoter activity of ICP4, ICP27 and
372 UL41 remained low (0.13, 0.03, 0.16, respectively) at a level similar to the negative control
373 promoters (0.27 and 0.15 for UL36 and UL45, respectively). In contrast, the promoter activity
374 of UL39 and UL49 reached high levels (3.5 and 5, respectively). These results indicate that
375 the ectopic overexpression of HIF-1α is sufficient to transactivate UL39 and UL49 promoters
376 and to induce a strong expression of a reporter gene, but insufficient to efficiently
377 transactivate ICP4, ICP27 and UL41 promoters.
378
379 ***Caspase 3/7-mediated apoptosis observed in hypoxia does not promote MDV reactivation*.**
380 HIF-1 was involved in the regulation of apoptosis pathways [37] and caspase activities was
381 shown to promote latent-to-lytic switch and/or viral replication [38]. Therefore, we next
382 explored whether the apoptosis induced under hypoxia could favor MDV reactivation
383 indirectly through caspases activation. We focused on caspase 3, a final effector in apoptotic
384 death. First, we validated Z-DEVD-FMK as a caspase 3 inhibitor on 3867K cells, showing
385 "physiological" apoptosis in normoxia (Table 1), using the luminescent Caspase-Glo® 3/7
386 assay. 3867K cells treated with 50µM of Z-DEVD-FMK for 24 h in normoxia showed a caspase
387 3/7 activity significantly reduced of 92.5-fold compared to in its absence (Figure 10A). Next,
388 3867K cells were cultivated in hypoxia for 72 h in presence or absence of Z-DEVD-FMK
389 (50µM), with Z-DEVD-FMK renewal every 24 h. After 48 h and 72 h, caspase 3/7 activity was
390 assayed in parallel to cell mortality and MDV reactivation by flow cytometry as previously
391 used. In the presence of Z-DEVD-FMK under hypoxia, the caspase 3/7 activity was
392 significantly reduced of 135-fold at 48 h and of 421-fold at 72h (Figure 10B). At 48h,

reactivated cells (GFP-positive cells) represented 4.1% of the live cells treated with Z-DEVD-FMK, close to the 3.4% measured for Z-DEVD-FMK-untreated cells (Figure 10B, left panel). At 72 h, the percentage of GFP-positive cells raised up to 6.4% with Z-DEVD-FMK, a rate comparable to the 5.4% observed without Z-DEVD-FMK (Figure 10B, right panel). The results thus indicate that MDV reactivation upon hypoxia is not promoted by caspase 3/7 activity in the 3867K cell line.

DISCUSSION

This is the first study showing that acute hypoxia launches MDV lytic cycle from latently infected T-lymphocytes derived from MD-lymphomas. Previous studies had shown a reactivation effect of hypoxia on gamma-herpesviruses from latently infected B-cells [4-6]. Here we showed the reactivation of an alpha-herpesvirus, indicating that hypoxia may be a reactivation stimulus shared by several herpesvirus subfamilies. As for most herpesviruses, EBV, KSHV, and MHV-4 persist as episome in latency [39], whereas MDV integrates in the cellular genome, preferentially in the telomeres [19-21]. Therefore, having a latent episomal form is not a condition necessary for herpesvirus reactivation by hypoxia. In this study, we detected reactivation only in a subset of the cells exposed to hypoxia or treated with chemicals stabilizing HIF-1α in normoxia. This result is consistent with previous reports on gamma-herpesviruses. Indeed, Davis et al. reported less than 3% KSHV-reactivating cells among BC-3 and BCBL-1 exposed to 1% O_2 during 48 to 72 h [4]. Polcicova et al. reported a much higher reactivation rate (52%) for MHV-4 from NB-78 cells exposed to 2% O_2 for 72 h [6]. However, these cells also exhibited an unusual spontaneous reactivation level of 7%. Kraus et al. also reported EBV

reactivation in a subset of HIF-1α -positive cells treated with deferoxamine (DFO), an agent mimicking hypoxia like MLN4924 [7]. In addition, this feature of partial reactivation was also observed when MD derived T-cells were treated *in vitro* with pharmacological agents acting through different mechanisms, for instance modifications of the chromatin structure (*eg,* with sodium butyrate) [40], alterations of DNA integrity, or replication (*eg,* with etoposide, 5-iododexoxyuridine) [41, 42]. Why all the cells in a "clonal" population do not reactivate after exposure to a reactivation stimulus is currently unknown. Single-cell RNA sequencing may enable answer this question.

Herein, virus reactivation was detected based on viral lytic genes expression and viral DNA quantification, as always performed for MDV. Because MDV replication in culture results only in 0.1% intracellular mature virions in 3867 K [34] with no extracellular virions detectable, we could not measure whether reactivation in hypoxia led to a productive cycle with mature virions.

Besides reactivation, hypoxia was associated with high cell mortality, particularly with MSB-1 cells. Such mortality levels were unexpected because hypoxia is a hallmark of most human solid tumors [29], including lymphomas [43]. Depending on the cell type, hypoxia can have opposing effects on cell death, especially apoptosis [44]. While numerous cells establish apoptosis protection mechanisms when exposed to hypoxia [45], some remain sensitive to apoptosis. For example, hypoxia induces apoptosis in the human oral squamous cell carcinoma cell line (OSC-4) [46] and in primary rat fibroblasts transformed by Ras and Myc oncogenes [47]. Therefore, one can wonder if the phenotype observed herein with MSB-1 and 3867K cell lines is peculiar to these cell lines or a common feature of MD-lymphomas derived cells. In our study, four possible mechanisms may have

441 contributed to cell death in hypoxia: first, hypoxia may have caused a global metabolic
442 and oxidative cellular stress due to a lack of ATP, mitochondria damages, or reactive
443 oxygen species [ROS] production. Hypoxia triggers HIF-1 stabilization, which is known to
444 activate NOX and iNOS genes [48], potentially leading to apoptosis [49]. Second, hypoxia
445 may have caused a glucose/nutrient shortage, which is highly toxic for cells [50]. Because
446 the medium was not renewed during the 72-96 h of hypoxia, we cannot rule out that cells
447 had consumed most of the glucose/nutrients, and had lacked glucose/nutrients in
448 addition to O_2 at some time points. Third, hypoxia may have caused the premature
449 expression of a viral cytotoxic protein. Indeed, UL49, considered a 'late' viral gene was
450 upregulated after only 24 h of hypoxia. UL49 encodes VP22, a tegument protein essential
451 for MDV replication that triggers DNA damage in proliferating cells when ectopically
452 expressed [51]. Fourth, the lytic cycle itself could have led to cell death, notably at 72 and
453 96 h. This last hypothesis is the less probable as sorted-dead cells did not express lytic
454 antigens after 48h in hypoxia as shown in figure 1C.
455 We observed MDV reactivation in normoxia in 3867K cells with $CoCl_2$ and MLN4924, two
456 molecules known to mimic hypoxia in numerous mammalian cells by stabilizing HIF-1α.
457 Treatment with these chemicals for 24 h induced 2- to 4-fold MDV reactivation compared
458 to mock-treated cells. This is comparable to the level of KSHV reactivation (5-fold, based
459 on gpK8.1 lytic protein expression) in BCBL-1 treated with 100 mM $CoCl_2$ for 72 h [4]. EBV
460 reactivation into lytic infection and HIF-1α stabilization has been reported with various
461 hypoxia mimicking molecules, including MLN4924, in the EBV+ GV-derived cell lines [7].
462 Although HIF-1α was detected (albeit at a low level) in all MLN4924-treated cells, it
463 remains unclear whether MDV reactivation was due to HIF-1 stabilization. Indeed, we did
464 not observe an upregulation of the HIF-1 glycolytic target genes, suggesting that HIF-1

465 may not be sufficiently expressed or was missing a cofactor (for *e.g.* p300/CBP) to be fully
466 functional [52]. Thus we suspect that the reactivation observed with MLN4924 could also
467 be independent of HIF-1α. MLN4924 is known to induce deregulation of the S-phase DNA
468 synthesis in tumoral cells with rapid cell division [53] and induce DNA double-strand
469 breaks (DSBs) [54]. As we have previously shown that induction of DNA DSBs triggers
470 reactivation in 3867K cells [42], we suspected that the reactivation with MLN4924 could
471 also be due to this molecular mechanism.

472 We demonstrated that hHIF-1α is functional in two chicken cell lines when overexpressed.
473 Our result therefore indirectly indicates that the hHIF-1α can dimerize with the chicken HIF-
474 1ß. Nevertheless, despite the HRE conservation in vertebrates and the high amino acid
475 identity of 79% between the chicken and human HIF-1α proteins [55], it cannot be certified
476 that hHIF-1α is fully as efficient as its chicken counterpart for MDV reactivation.

477 Although we clearly demonstrated that HIF-1α expression triggers MDV reactivation in
478 MSB-1 cells, the molecular pathway initiating MDV reactivation remains puzzling. Ectopic
479 expression of hHIF-1α (WT and stabilized) led to reactivation of 3.25% of the cells 24 h
480 post-transfection, which is consistent with the percentage of MSB-1 cells reactivated after
481 24 h under hypoxia (3.16%). However, the fact that HIF-1α WT led to the same
482 reactivation efficacy than the stabilized HIF-1α mutant is surprising, because HIF-1α WT
483 was less effective than the stabilized HIF-1α at transactivating the reporter gene (EGFP
484 destabilized protein). One possible explanation is a 'hit-and-run' mechanism, whereby WT
485 HIF-1 is expressed, triggering the lytic cycle in some cells, but its too transient expression
486 makes it undetectable at the time of cell fixation. A similar observation was made in EBV+
487 GC derived-cells treated with DFO for 24 h; after DFO removal, cells had lost HIF-1α

488 expression but were still in lytic cycle [7]. Another unexpected result was that only 0.9%
489 and 0.2% of the reactivated cells were HIF-1α-positive by immunofluorescence after
490 transfection with stabilized or WT HIF-1α, respectively. Although these percentages are
491 possibly slightly underestimated (immunofluorescence being less sensitive at detecting
492 HIF-1α expression than the reporter assay), this result indicates that the effect of HIF-1 on
493 reactivation may be direct and/or indirect. If here again a hit and run mechanism can be
494 possible, another plausible hypothesis is an indirect effect of HIF-1. Indeed, HIF-1 is known
495 to activate more than 100 cellular genes in mammals [56], including secreted proteins and
496 adhesion molecules. In addition, hypoxia and HIF-1 stimulate the production of cellular
497 exosomes and modify their contents [57]. Therefore, one or several cellular components
498 released in the extracellular environment during hypoxia may play a “pro-reactivation”
499 role on the neighboring cells.
500 During hypoxia, MDV reactivation was accompanied by an increased transcription of all
501 sixteen lytic genes monitored, some of which exhibiting putative HREs in their promoter
502 regions. Among these sixteen lytic genes, six were overexpressed both in 3867K and MSB-
503 1 under hypoxia, which makes them susceptible to be targeted by HIF-1. The presence of
504 1 to 3 HREs in the promoter region of these six genes in RB-1B and Md5 is consistent with
505 this interpretation. The fact that only a few genes harboring one or several HREs are
506 overexpressed in hypoxia is not surprising. Indeed, in mammalian cells, only 1% of the
507 cellular HREs were found to bind HIF-1 by chip assay after hypoxia exposure [56].
508 In gamma-herpesviruses, a single IE gene regulates the latent-to-lytic switch: ORF50-rta
509 for KSHV and MHV-4 and BZLF1 for EBV. These genes are transcriptionally activated by
510 HIF-1 [6-9]. We reasoned that this molecular mechanism could also trigger MDV
511 reactivation in hypoxia. In that perspective, *ICP4* is of particular interest as it is considered

512 as a potential initiator of the lytic cycle, although this has not been demonstrated. Our
513 data from the promoter assay showed that the overexpression of the stabilized hHIF-1α in
514 normoxia increases the basal activity of the ICP4 promoter, but which remained low, close
515 to the basal activity of promoters lacking HRE. This result suggests that the upregulation
516 of ICP4 observed in hypoxia is independent of the HRE present in its promoter and might
517 rely on other cellular or viral factors induced upon hypoxic conditions. Interestingly the
518 promoter assay showed a clear upregulation of UL39 and UL49 promoters activity by HIF-
519 1, which is in accordance with the transcripts expression after 24h of hypoxia in both cell
520 lines. How UL39 expression could contribute to MDV reactivation is unclear. As previously
521 reported for HSV-1, we can speculate that the large ribonucleotide reductase subunit
522 encoded by UL39 might contribute to the lytic switch of MDV as an auxiliary factor in the
523 viral DNA replication machinery [58]. Moreover, it was shown that UL39 mutants are
524 severely impaired for replication, establishment of latency and reactivation in murine
525 models of HSV-1 [59]. About UL49, its role in MDV reactivation under hypoxia is very
526 plausible. Indeed, we demonstrated earlier that MDV VP22 triggers DNA damages in
527 proliferating cells [51] and that induction of DNA damages with chemicals triggers MDV
528 reactivation in 3867K cells [42]. Further studies are needed to explore the role of UL49 in
529 this process, for example by mutating HREs in UL49 promoter or by ChiP assay to
530 demonstrate the binding of HIF-1 to UL49 promoter in hypoxia.
531 For some herpesviruses, caspase activities were shown to promote latent-to-lytic switch
532 and/or viral replication [38]. For example, caspase-mediated cleavage of PIAS1
533 contributes to EBV reactivation from B-cells [60]. HIF-1 being involved in the regulation of
534 apoptosis pathways [37], and a high cell death of MDV-latently infected T-cells having
535 been observed herein under hypoxia, a role of caspases in MDV reactivation was possible,

although never been explored before. We found that inhibition of caspase 3/7 activity does not impact MDV reactivation in 3867K cultured for 48/72 h in hypoxia. This result suggests that MDV reactivation triggered in hypoxia is independent of the caspase 3/7 activation and more likely relies on other mechanisms, discussed above.

Taken together, we demonstrate for the first time that hypoxia can trigger MDV reactivation from transformed latently infected T-cells. With late immunodepression, hypoxia is a physiological trigger of reactivation, which could explain the second lytic phase observed during the Marek's disease *in vivo*. We also demonstrated that overexpression of HIF1α (WT or an oxygen insensitive mutant) is sufficient to induce MDV reactivation in normoxia. Thus, hypoxia and HIF-1α are new triggers of MDV reactivation.

MATERIAL AND METHODS

Cells.

Two MDV-transformed lymphoblastoid T-cell lines were used: the 3867K cell line, derived from a kidney lymphoma induced by the very virulent mutant rRB-1B UL47eGFP [34] ; the MSB-1 cell line, derived from a spleen lymphoma induced by a virulent strain of BC1 GaHV-2 strain [32, 33]. The MSB-1 has been used extensively for the analysis of MDV latency and latent-to-lytic switch [61]. 3867K cells were cultured and maintained as previously described [34]. MSB-1 cells were cultured in RPMI 1640 supplemented with 2 mM of glutamine and 10% fetal bovine serum. In normoxia, both cell lines were grown at 41°C in a standard incubator in atmospheric O_2 (21% O_2 v/v), with 5% CO_2.

ESCDL-1 cell line used for promoter transactivation assays was cultivated as previously described [62].

Antibodies.

Anti-HIF-1α (rabbit polyclonal) was obtained from Novus Biologicals (NB 100-449) and used at 1:100e in immunostaining. Mouse monoclonal antibodies directed against MDV lytic antigens gB (clone K11; 1:1000e), VP22 (clone B17; 1:300e) and ICP4 (clone E21; 1:1000e) were previously described [63, 64] and used at dilution indicated above. As secondary antibodies, goat anti-rabbit (GAR) Alexa Fluor 594 or 488 (ThermoFisher Scientific) and goat anti-mouse (GAM) Alexa Fluor 555 or 594 or 488 (ThermoFisher Scientific) were used.

Plasmids.

The pPB tdTomato, a kind gift from Bertrand Pain, is a modified PiggyBac vector (obtained from Austin Smith laboratory, Cambridge, UK) expressing the tdTomato fluorescent gene driven by a CAG promoter. This vector was used for measuring transfection efficiencies. The pHRE-d2EGFP, a kind gift of Martin Brown and Thomas Foster, is a hypoxia reporter plasmid, encoding the destabilized Enhanced Green Fluorescent Protein (EGFP) under the control of hCMV minimal promoter, located downstream of five HRE from *vEGF* gene (vascular Endothelial Growth Factor) (Addgene plasmid# 46926, http://n2t.net/addgene:46926 ; RRID:Addgene_46926) [65]. The pHRE-d2EGFP was used as a reporter gene of HIF-1 activity. The HA-HIF1α WT- pcDNA3, a kind gift from William Kaelin (Addgene plasmid # 18949 ; http://n2t.net/addgene:18949 ; RRID:Addgene_18949) is a CMV promoter-driven vector expressing the human wild-type (WT) form of HIF-1α [66]. The HA-HIF1α P402A/P564A/N803A-pcDNA3, a kind gift from William Kaelin (Addgene plasmid # 87261 ; http://n2t.net/addgene:87261 ; RRID:Addgene_87261) is a CMV promoter-driven vector expressing a stabilized HIF-1α in which the three amino acids targeted by hydroxylation were mutated [67]. The mutant protein is O_2 insensitive and thus resistant to proteasomal-

584 specific degradation under normoxic conditions. The HA-HIF1α WT- pcDNA3 and the HIF1α
585 P402A/P564A/N803A-pcDNA3 plasmids were used for HIF-1 α overpression in normoxia.
586
587 ***Cell culture in hypoxia.***
588 Cells were seeded at $2x10^6$ cells per mL in normoxia. One hour after division, cells were
589 placed in a hypoxia workstation (HypoxyLab, Oxford Optronix, Abingdon, UK) at 1 % O_2 v/v
590 and 5 % CO_2 (hypoxia conditions) at 41°C, and incubated during 24 to 96 h. At the time of
591 introduction in the hypoxia chamber, the cell medium contained O_2 in order to permit a
592 progressive deprivation of O_2 over the first 24 h. Due to the rapid degradation of HIF-α at
593 21% O_2, all experimental steps until cell fixation or lysis were performed within the
594 hypoxia chamber.
595
596 ***Flow cytometry analyses and cell-sorting.***
597 For 3867K cells, MDV reactivation was detected directly with UL47eGFP fluorescence by flow
598 cytometry. For live/dead analyses or live cell-sorting, cells were stained with the Fixable
599 Viability Dye eFluor 780 (ThermoFisher Scientific) according to standard procedure before
600 fixation using 1% paraformaldehyde (PFA). Flow cytometry analyses were performed either
601 with a MoFlo Astrios^{EQ} flow cytometer (Beckman Coulter, Brea, USA) or with a FACS LSR
602 Fortessa cytometer (Becton Dickinson, Heidelberg, Germany). For the FACS LSR Fortessa
603 cytometer, acquisition was performed with BD FACSDiva software and analyzed with FlowJo
604 software (FlowJo LLC, Ashland, USA).
605 After Fixable Viability Dye eFluor 780 staining and 1% PFA fixation, “live cells” were sort-
606 purified by FACS gating on eFluor 780 negative with a MoFlo Astrios^{EQ} flow cytometer
607 (Beckman Coulter, Brea, USA), whereas “dead cells” (eFluor 780-positive) were removed.

608

609 ***Immunostaining and fluorescence microscopy.***

610 Total cells or “live” sort-purified cells fixed in PFA were plated by centrifugation at low speed
611 (500 × g; 800rpm) for 5 min on 0.17µm-thick- glass coverslips using a Cytospin 4
612 (ThermoFisher Scientific). For MDV antigens and HIF-1α detection, the immunostainings
613 were performed for 1h in PBS, 0.1% Triton X-100, 1% bovine serum albumin (BSA). After
614 washes, the cells were incubated for 45 min with an appropriate secondary antibody(ies)
615 coupled to Alexa Fluor 488 or 555 or 594. Lastly, the nuclei were counterstained with
616 Hoechst 33342 dye (1:2000e) (Invitrogen) and the coverslips were mounted with Mowiol
617 (Merck). Such a procedure was used for cells cultivated in hypoxia, normoxia, treated with
618 pharmacological agents, as well as cells transfected with vectors expressing hHIF-1α.
619 Microscopic observations were performed using an Axiovert 200 M inverted epifluorescence
620 microscope equipped with an Apotome imaging system (Zeiss). Images were captured with
621 an AxioCam MRm charge-coupled-device camera (Zeiss) by using Axiovision software (Zeiss).
622 In several experiments, various subsets of cells were counted using Axiovision software on
623 captured images.

624

625 ***Fluorescence quantification***

626 The quantification of HIF-1 fluorescence was performed on high magnification digital
627 microscopy images using FIJI free software. First, images (HIF-1α red channel) were adjusted
628 in brightness/contrast with the Auto mode. A filter (median) was applied to all images. The
629 threshold of each image was applied with the default mode in order to visualize the cells
630 exhibiting a HIF-1α signal. The HIF-1α-positive fluorescent cells were selected with the
631 “analyze particles” tool, (small objects under 5µm were excluded). The mean grey value of

all selected cells was next measured (fluorescence measurement) and reported in an excel table. For images, on which cells were touching each other, after the threshold setting and before fluorescence measurement, cells were segmented one from the other by the “binary watershed” process.

Sequence analysis for HREs detection in MDV complete genome.

The putative HREs were identified in the MDV RB-1B complete genome (GenBank : EF523390) by using a bioinformatic approach with the "dreg" tool of EMBOSS 6.6.0.0 software (REF:10.1016/s0168-9525(00)02024-2). The command line "dreg" was used to locate in the entire genome all HREs on both strands by using the pattern “RCGTG”, where 'R' was either an A or a G nucleotide. A local python script (available on demand) was then used to compare positions of all identified HREs and positions of each known Coding DNA Sequence (CDS). Thus, HREs located within a range of -700 nt and +70 nt (assuming to encompass the promoter region) from the +1 of each CDS (+1 being the ‘A’ of the transcriptional starting codon) were retained and numerated.

Quantification of MDV genome copy number by real-time PCR (qPCR).

DNA was extracted from 10^7 cells (3867K or MSB-1) by using QIAmp DNA mini kit according to the manufacturer’s instructions (Qiagen). MDV genome was quantified using TaqMan technology, as previously described [27]. Briefly, for each sample, copy number of the viral *ICP4* gene and the cellular *iNOS* gene were quantified independently in triplicates, in parallel to standards. The positive cut-off points corresponded to 23 copies for *ICP4* and 57 copies for *iNOS*. For each sample, the number of MDV genome copies are given per 10^6 cells.

RNA isolation and reverse transcription qPCR (RT-qPCR).

RNAs were extracted from cells (3867K or MSB-1) by using the RNeasy mini kit (#74104, Qiagen), according to the manufacturer's recommendations. RNAs were treated with RNase-free RQ1 DNase (#M6101, Promega) and RNAs concentrations were measured with a Nanodrop spectrophotometer (ThermoFisher Scientific). Five hundred ng of total RNA was reverse-transcribed by using 50µg/ml oligo(dT) primers (#C110A, Promega), dNTP (#U151A, Promega) and Moloney MLV reverse-transcriptase (#M1701, Promega). The expression of genes of interest was measured by real-time qPCR with iQ Supermix SYBR green (#1708882, Bio-Rad) in triplicate on a C1000 Touch CFX96 Real-Time PCR Detection System (Bio-Rad). The primer used for the qPCRs (viral and cellular genes) were synthetized by Eurogentec and are listed in table 2. The chicken ribosomal protein S17 gene (RPS17) was used as the reference cellular housekeeping gene. The qPCR program consisted of a 5 min activation step at 95°C, followed by 40 cycles of 95°C for 20 sec and 60°C for 35 sec. The relative changes in gene expression were calculated relatively to the expression of the RPS17 and determined by the 2^{-DDct} threshold cycle (C_T) method.

Cell treatment with pharmacological agents.

Two hypoxia-mimicking pharmacological agents were used: MLN4924, a Nedd8-Activating Enzyme Inhibitor (Pevodistat #11260, AdooQ Bioscience) and $CoCl_2$, an iron chelator which prevents hydroxylases activity and the hydroxylation of HIF α subunit (#C8661, Sigma). The stock solutions were diluted at 2.5 mM in DMSO and 50 mM in water, respectively. 3867K cells (10^6 cells/mL) were incubated with various concentrations of MLN4924 or $CoCl_2$ for 24 h. Cells were next stained for live/dead and fixed for subsequent analyses by flow cytometry analyses or fluorescence microscopy. Sodium butyrate, an inhibitor of histone deacetylases

was used as a positive control of reactivation. The sodium butyrate stock solution was prepared at 100 mM in water and the cells treated with 0.5mM for 48 h.

Transient transfection and transactivation assay to monitor hHIF-1α functionality in MSB-1.

Cells (3867K and MSB-1) were transiently transfected by using a Neon® electroporation device system and the Neon transfection system 10µL kit, according to manufacturer's instructions (ThermoFisher Scientific). For each transfection, $5x10^5$ cells were mixed with 1µg of plasmid in 10µL of re-suspension buffer. When two plasmids were co-transfected 1µg of each was used. Cells were electroporated with the conditions optimized for the PB tdTomato, according to manufacturer's instructions. Cells transfected with an empty plasmid served as a negative control as well as mock-transfected cells (no plasmid). After electroporation, the cells were seeded in 48-well plates containing 250µL of culture medium. The cells were cultured for 24 h and subsequently proceeded for analysis.

In order to test the functionality of hHIF-1α (WT and mutant), MSB-1 were co-transfected as above with a hHIF-1α vector and the pHRE-d2EGFP plasmid. The cells were then fixed, plated on coverslips and counted to determine the percentage of GFP cells, as GFP expression is dependent on HIF-1α functionality.

Caspase 3 inhibitor treatment and Caspase-Glo® 3/7 assay.

3867K ($2x10^6$ cells/mL) were cultivated in hypoxia (1%) for 72 h, with or without 50µM of Z-DEVD-FMK caspase 3 inhibitor (FMK004, R&D systems) in a 6-well plate. The Z-DEVD-FMK stock solution was diluted in DMSO at 20mM. The Z-DEVD-FMK treatment (50µM) was renewed every 24 h as well as DMSO, in the mock-treated cells. As controls, we also used

cells in normoxia, treated and non-treated with Z-DEVD-FMK. At 48 h and 72 h of culture, luminescent caspase 3/7 activation assay was performed according to the manufacturer's instructions (Caspase-Glo® 3/7 assay, Promega). Briefly, 50µl of cells treated or not (in duplicate) were transferred in a white opaque 96-well plate, lysed and incubated at room temperature for 1 h with Caspase-Glo® reagent. It should be noted that the cells maintained in hypoxia were lysed in the hypoxia chamber, then taken out of the chamber for the room temperature incubation. The luciferase activity related to the enzymatic activity of caspase-3/7 was next measured using a GloMax-Multi Detection System (Promega).

Promoters cloning and promoter activity after HIF-1α over-expression in normoxia.

The promoter regions of ICP4, ICP27, UL39, UL41, UL49 as well as UL36 and UL45 were amplified by PCR from the RB-1B BAC using the Phusion Taq (NEB) and the primers depicted in Table 3. UL36 and UL45 promoters lacking HRE on both DNA strands were used as MDV negative control promoters. The amplified sequences were inserted into the XhoI/HindIII sites upstream of a destabilized firefly luciferase gene in the pGL4.11 [*luc2P*] vector (#E666A; Promega). ESCDL-1 cells were seeded on a 96-well plate ($2.5x10^4$ cells/well) 20 h before transfection. Cells were co-transfected with 200ng of each pGL4.11 promoter construct and 10 ng of a pTK Renilla Luc (pRL). For the condition where HIF1α is overexpressed, 200ng of the HA-HIF1α P402A/P564A/N803A-pcDNA3 vector was co-transfected together with the reporter plasmid and pRL. Each condition was performed in quintuplicate, in two independent experiments. At 24 h post-transfection, Renilla and Firefly luciferases activities were measured using the dual luciferase reporter assay system (#E1910, Promega) following the manufacturers' instructions and the GloMax-Multi Detection System (Promega). Firefly luciferase activities were normalized with respect to Renilla luciferase activity.

Statistical analysis.

Comparison of two groups was performed by a Mann-Whitney test. Comparison of proportions were performed by the Chi2 test or by the Fisher exact test, when the Chi2 test was not applicable due to limited number of individuals. GraphPad prism version 7, Anastats free softwares (https://www.anastats.fr/telechargements/) or the R software version 3.6.0 were used for plots and computing.

ACKNOWLEDGMENTS

The authors would like to thank Yves Le Vern (INRAE, Nouzilly, France) for cell-sorting by flow cytometry, Dr Venugopal Nair (The Pirbright Institute, UK) for providing the 3867K cells, Dr Bertrand Pain (Stem-cell and Brain Research Institute, Lyon, France) for providing the pPB tdTomato, Dr Fréderic Mazurier for discussions (IDGR, Rennes, France), Dr Gilles Le Pape for discussions on statistical analyses and Addgene (Watertown, Mass., USA) for providing plasmids. C.M. was supported by a French MESRI PhD fellowship.

REFERENCES

1. Roizman B (2013) Herpesviridae. In: Knipe D.M., Howley P.M. (eds.) Fields Virology. Lippincott Williams & Wilkins, Philadelphia, pp. 1802-1822
2. Roizman B, Whitley RJ (2013) An inquiry into the molecular basis of HSV latency and reactivation. Annu Rev Microbiol 67:355-374
3. Stowe RP, Kozlova EV, Yetman DL, Walling DM, Goodwin JS, Glaser R (2007) Chronic herpesvirus reactivation occurs in aging. Exp Gerontol 42:563-570
4. Davis DA, Rinderknecht AS, Zoeteweij JP, Aoki Y, Read-Connole EL, Tosato G, Blauvelt A, Yarchoan R (2001) Hypoxia induces lytic replication of Kaposi sarcoma-associated herpesvirus. Blood 97:3244-3250
5. Jiang JH, Wang N, Li A, Liao WT, Pan ZG, Mai SJ, Li DJ, Zeng MS, Wen JM, Zeng YX (2006) Hypoxia can contribute to the induction of the Epstein-Barr virus (EBV) lytic cycle. J Clin Virol 37:98-103

6. Polcicova K, Hrabovska Z, Mistrikova J, Tomaskova J, Pastorek J, Pastorekova S, Kopacek J (2008) Up-regulation of Murid herpesvirus 4 ORF50 by hypoxia: possible implication for virus reactivation from latency. Virus Res 132:257-262
7. Kraus RJ, Yu X, Cordes BA, Sathiamoorthi S, Iempridee T, Nawandar DM, Ma S, Romero-Masters JC, McChesney KG, Lin Z, Makielski KR, Lee DL, Lambert PF, Johannsen EC, Kenney SC, Mertz JE (2017) Hypoxia-inducible factor-1alpha plays roles in Epstein-Barr virus's natural life cycle and tumorigenesis by inducing lytic infection through direct binding to the immediate-early BZLF1 gene promoter. PLoS Pathog 13:e1006404
8. Haque M, Davis DA, Wang V, Widmer I, Yarchoan R (2003) Kaposi's sarcoma-associated herpesvirus (human herpesvirus 8) contains hypoxia response elements: relevance to lytic induction by hypoxia. J Virol 77:6761-6768
9. Cai Q, Lan K, Verma SC, Si H, Lin D, Robertson ES (2006) Kaposi's sarcoma-associated herpesvirus latent protein LANA interacts with HIF-1 alpha to upregulate RTA expression during hypoxia: Latency control under low oxygen conditions. J Virol 80:7965-7975
10. Semenza GL (2003) Targeting HIF-1 for cancer therapy. Nat Rev Cancer 3:721-732
11. Loenarz C, Coleman ML, Boleininger A, Schierwater B, Holland PW, Ratcliffe PJ, Schofield CJ (2011) The hypoxia-inducible transcription factor pathway regulates oxygen sensing in the simplest animal, Trichoplax adhaerens. EMBO Rep 12:63-70
12. Brahimi-Horn MC, Pouyssegur J (2009) HIF at a glance. J Cell Sci 122:1055-1057
13. Huang LE, Gu J, Schau M, Bunn HF (1998) Regulation of hypoxia-inducible factor 1alpha is mediated by an O2-dependent degradation domain via the ubiquitin-proteasome pathway. Proc Natl Acad Sci U S A 95:7987-7992
14. Bruick RK, McKnight SL (2001) A conserved family of prolyl-4-hydroxylases that modify HIF. Science 294:1337-1340
15. Kaelin WG, Jr., Ratcliffe PJ (2008) Oxygen sensing by metazoans: the central role of the HIF hydroxylase pathway. Mol Cell 30:393-402
16. Calnek BW (1998) Lymphomagenesis in Marek's Disease. Avian Pathol 27:S54-S64
17. Schat KA, Nair V (2008) Marek's Disease. In: Saif Y.M. (ed) Disease of Poultry. Blackwell Publishing Ltd, Ames, pp. 452-514
18. Calnek BW (1986) Marek's disease--a model for herpesvirus oncology. Crit Rev Microbiol 12:293-320
19. Delecluse HJ, Hammerschmidt W (1993) Status of Marek's disease virus in established lymphoma cell lines: herpesvirus integration is common. J Virol 67:82-92
20. Kaufer BB, Jarosinski KW, Osterrieder N (2011) Herpesvirus telomeric repeats facilitate genomic integration into host telomeres and mobilization of viral DNA during reactivation. J Exp Med 208:605-615
21. Osterrieder N, Wallaschek N, Kaufer BB (2014) Herpesvirus Genome Integration into Telomeric Repeats of Host Cell Chromosomes. Annu Rev Virol 1:215-235
22. Jones D, Lee L, Liu JL, Kung HJ, Tillotson JK (1992) Marek disease virus encodes a basic-leucine zipper gene resembling the fos/jun oncogenes that is highly expressed in lymphoblastoid tumors. Proc Natl Acad Sci U S A 89:4042-4046
23. Cantello JL, Anderson AS, Morgan RW (1994) Identification of latency-associated transcripts that map antisense to the ICP4 homolog gene of Marek's disease virus. J Virol 68:6280-6290

24. Cantello JL, Parcells MS, Anderson AS, Morgan RW (1997) Marek's disease virus latency-associated transcripts belong to a family of spliced RNAs that are antisense to the ICP4 homolog gene. J Virol 71:1353-1361
25. Burnside J, Bernberg E, Anderson A, Lu C, Meyers BC, Green PJ, Jain N, Isaacs G, Morgan RW (2006) Marek's disease virus encodes MicroRNAs that map to meq and the latency-associated transcript. J Virol 80:8778-8786
26. Yao Y, Zhao Y, Xu H, Smith LP, Lawrie CH, Watson M, Nair V (2008) MicroRNA profile of Marek's disease virus-transformed T-cell line MSB-1: predominance of virus-encoded microRNAs. J Virol 82:4007-4015
27. Rémy S, Blondeau C, Le Vern Y, Lemesle M, Vautherot J-F, Denesvre C (2013) Fluorescent tagging of VP22 in N-terminus reveals that VP22 favors Marek's disease virus virulence in chickens and allows morphogenesis study in MD tumor cells. Vet Res 44:125
28. Parcells MS, Arumugaswami V, Prigge JT, Pandya K, Dienglewicz RL (2003) Marek's disease virus reactivation from latency: changes in gene expression at the origin of replication. Poult Sci 82:893-898
29. Fleming IN, Manavaki R, Blower PJ, West C, Williams KJ, Harris AL, Domarkas J, Lord S, Baldry C, Gilbert FJ (2015) Imaging tumour hypoxia with positron emission tomography. Br J Cancer 112:238-250
30. Vaupel P, Kallinowski F, Okunieff P (1989) Blood flow, oxygen and nutrient supply, and metabolic microenvironment of human tumors: a review. Cancer Res 49:6449-6465
31. Bertout JA, Patel SA, Simon MC (2008) The impact of O2 availability on human cancer. Nat Rev Cancer 8:967-975
32. Akiyama Y, Kato A (1973) Continuous cell culture from lymphoma of Marek's disease. Biken Journal 16:177-179
33. Akiyama Y, Kato S (1974) Two cell lines from lymphomas of Marek's disease. Biken J 17:105-116
34. Denesvre C, Rémy S, Fragnet L, Smith LP, Georgeault S, Vautherot J-F, Nair V (2016) Marek's disease virus undergoes complete morphogenesis after reactivation in T-lymphoblastoid cell line transformed by recombinant fluorescent marker virus. J. Gen. Virol. 97:480-486
35. Jarosinski KW, Arndt S, Kaufer BB, Osterrieder N (2012) Fluorescently tagged pUL47 of Marek's disease virus reveals differential tissue expression of the tegument protein in vivo. J Virol 86:2428-2436
36. Spatz SJ, Zhao Y, Petherbridge L, Smith LP, Baigent SJ, Nair V (2007) Comparative sequence analysis of a highly oncogenic but horizontal spread-defective clone of Marek's disease virus. Virus Genes 35:753-766
37. Greijer AE, van der Wall E (2004) The role of hypoxia inducible factor 1 (HIF-1) in hypoxia induced apoptosis. J Clin Pathol 57:1009-1014
38. Tabtieng T, Gaglia MM (2018) Emerging Proviral Roles of Caspases during Lytic Replication of Gammaherpesviruses. J Virol 92
39. Lieberman PM (2016) Epigenetics and Genetics of Viral Latency. Cell Host Microbe 19:619-628
40. Brown AC, Nair V, Allday MJ (2012) Epigenetic regulation of the latency-associated region of Marek's disease virus in tumor-derived T-cell lines and primary lymphoma. J Virol 86:1683-1695

41. Parcells MS, Dienglewicz RL, Anderson AS, Morgan RW (1999) Recombinant Marek's disease virus (MDV)-derived lymphoblastoid cell lines: regulation of a marker gene within the context of the MDV genome. J Virol 73:1362-1373
42. Bencherit D, Rémy S, Le Vern Y, Vychodil T, Bertzbach LD, Kaufer BB, Denesvre C, Trapp-Fragnet L (2017) Induction of DNA damages upon Marek's disease virus infection: implication in viral replication and pathogenesis. J. Virol. 91:1-36
43. Postema EJ, McEwan AJ, Riauka TA, Kumar P, Richmond DA, Abrams DN, Wiebe LI (2009) Initial results of hypoxia imaging using 1-alpha-D: -(5-deoxy-5-[18F]-fluoroarabinofuranosyl)-2-nitroimidazole (18F-FAZA). Eur J Nucl Med Mol Imaging 36:1565-1573
44. Sendoel A, Hengartner MO (2014) Apoptotic cell death under hypoxia. Physiology (Bethesda) 29:168-176
45. Chiche J, Rouleau M, Gounon P, Brahimi-Horn MC, Pouyssegur J, Mazure NM (2010) Hypoxic enlarged mitochondria protect cancer cells from apoptotic stimuli. J Cell Physiol 222:648-657
46. Sasabe E, Tatemoto Y, Li D, Yamamoto T, Osaki T (2005) Mechanism of HIF-1alpha-dependent suppression of hypoxia-induced apoptosis in squamous cell carcinoma cells. Cancer Sci 96:394-402
47. Schmaltz C, Hardenbergh PH, Wells A, Fisher DE (1998) Regulation of proliferation-survival decisions during tumor cell hypoxia. Mol Cell Biol 18:2845-2854
48. Tafani M, Sansone L, Limana F, Arcangeli T, De Santis E, Polese M, Fini M, Russo MA (2016) The Interplay of Reactive Oxygen Species, Hypoxia, Inflammation, and Sirtuins in Cancer Initiation and Progression. Oxid Med Cell Longev 2016:3907147
49. Redza-Dutordoir M, Averill-Bates DA (2016) Activation of apoptosis signalling pathways by reactive oxygen species. Biochim Biophys Acta 1863:2977-2992
50. Carmeliet P, Dor Y, Herbert JM, Fukumura D, Brusselmans K, Dewerchin M, Neeman M, Bono F, Abramovitch R, Maxwell P, Koch CJ, Ratcliffe P, Moons L, Jain RK, Collen D, Keshert E (1998) Role of HIF-1alpha in hypoxia-mediated apoptosis, cell proliferation and tumour angiogenesis. Nature 394:485-490
51. Trapp-Fragnet L, Bencherit D, Chabanne-Vautherot D, Le Vern Y, Rémy S, Boutet-Robinet E, Mirey G, Vautherot JF, Denesvre C (2014) Cell cycle modulation by Marek's disease virus: the tegument protein VP22 triggers S-phase arrest and DNA damage in proliferating cells. PLoS One 9:e100004
52. Kallio PJ, Okamoto K, O'Brien S, Carrero P, Makino Y, Tanaka H, Poellinger L (1998) Signal transduction in hypoxic cells: inducible nuclear translocation and recruitment of the CBP/p300 coactivator by the hypoxia-inducible factor-1alpha. EMBO J 17:6573-6586
53. Soucy TA, Smith PG, Milhollen MA, Berger AJ, Gavin JM, Adhikari S, Brownell JE, Burke KE, Cardin DP, Critchley S, Cullis CA, Doucette A, Garnsey JJ, Gaulin JL, Gershman RE, Lublinsky AR, McDonald A, Mizutani H, Narayanan U, Olhava EJ, Peluso S, Rezaei M, Sintchak MD, Talreja T, Thomas MP, Traore T, Vyskocil S, Weatherhead GS, Yu J, Zhang J, Dick LR, Claiborne CF, Rolfe M, Bolen JB, Langston SP (2009) An inhibitor of NEDD8-activating enzyme as a new approach to treat cancer. Nature 458:732-736
54. Brown JS, Jackson SP (2015) Ubiquitylation, neddylation and the DNA damage response. Open Biol 5:150018

55. Takahashi T, Sugishita Y, Nojiri T, Shimizu T, Yao A, Kinugawa K, Harada K, Nagai R (2001) Cloning of hypoxia-inducible factor 1alpha cDNA from chick embryonic ventricular myocytes. Biochem Biophys Res Commun 281:1057-1062
56. Mole DR, Blancher C, Copley RR, Pollard PJ, Gleadle JM, Ragoussis J, Ratcliffe PJ (2009) Genome-wide association of hypoxia-inducible factor (HIF)-1alpha and HIF-2alpha DNA binding with expression profiling of hypoxia-inducible transcripts. J Biol Chem 284:16767-16775
57. Choudhry H, Harris AL (2018) Advances in Hypoxia-Inducible Factor Biology. Cell Metab 27:281-298
58. Packard JE, Dembowski JA (2021) HSV-1 DNA Replication-Coordinated Regulation by Viral and Cellular Factors. Viruses 13
59. Mostafa HH, Thompson TW, Konen AJ, Haenchen SD, Hilliard JG, Macdonald SJ, Morrison LA, Davido DJ (2018) Herpes Simplex Virus 1 Mutant with Point Mutations in UL39 Is Impaired for Acute Viral Replication in Mice, Establishment of Latency, and Explant-Induced Reactivation. J Virol 92
60. Zhang K, Lv DW, Li R (2017) B Cell Receptor Activation and Chemical Induction Trigger Caspase-Mediated Cleavage of PIAS1 to Facilitate Epstein-Barr Virus Reactivation. Cell Rep 21:3445-3457
61. Morgan RW, Xie Q, Cantello JL, Miles AM, Bernberg EL, Kent J, Anderson A (2001) Marek's disease virus latency. Curr Top Microbiol Immunol 255:223-243
62. Vautherot JF, Jean C, Fragnet-Trapp L, Remy S, Chabanne-Vautherot D, Montillet G, Fuet A, Denesvre C, Pain B (2017) ESCDL-1, a new cell line derived from chicken embryonic stem cells, supports efficient replication of Mardiviruses. PLoS One 12:e0175259
63. Dorange F, El Mehdaoui S, Pichon C, Coursaget P, Vautherot JF (2000) Marek's disease virus (MDV) homologues of herpes simplex virus type 1 UL49 (VP22) and UL48 (VP16) genes: high-level expression and characterization of MDV-1 VP22 and VP16. J Gen Virol 81:2219-2230.
64. Blondeau C, Chbab N, Beaumont C, Courvoisier K, Osterrieder N, Vautherot J-F, Denesvre C (2007) A full UL13 open reading frame in Marek's disease virus (MDV) is dispensable for tumor formation and feather follicle tropism and cannot restore horizontal virus transmission of rRB-1B in vivo. Vet Res 38:419-433
65. Vordermark D, Shibata T, Brown JM (2001) Green fluorescent protein is a suitable reporter of tumor hypoxia despite an oxygen requirement for chromophore formation. Neoplasia 3:527-534
66. Kondo K, Klco J, Nakamura E, Lechpammer M, Kaelin WG, Jr. (2002) Inhibition of HIF is necessary for tumor suppression by the von Hippel-Lindau protein. Cancer Cell 1:237-246
67. Yan Q, Bartz S, Mao M, Li L, Kaelin WG, Jr. (2007) The hypoxia-inducible factor 2alpha N-terminal and C-terminal transactivation domains cooperate to promote renal tumorigenesis in vivo. Mol Cell Biol 27:2092-2102

939 **FIGURE LEGENDS**

940 **Figure 1. Hypoxia induces MDV reactivation in 3867K, a T-cell line latently infected with**
941 **RB-1B UL47eGFP**. (A) Viral reactivation and mortality. 3867K cells were cultivated for 72 h in
942 normoxia or hypoxia (1% O_2). Viral reactivation and mortality were analyzed by flow
943 cytometry. Reactivation was measured directly through the UL47eGFP signal, a protein
944 expressed in lytic cycle, whereas mortality was visualized with the fixable viability dye
945 eFluor780. The percentage of cells in lytic cycle and of dead cells (eFluor780-positive) is
946 given in hypoxia and normoxia relatively to the total cell number. The mean of green
947 fluorescence for latently-infected cells and cells in lytic cycle is also shown in green on the
948 bottom of both diagrams in arbitrary unit. (B) Images of 3867K cultivated in normoxia and
949 hypoxia for 72 h observed by fluorescence microscopy. The cells were stained with an
950 antibody recognizing VP22 or gB lytic proteins (red), in addition to UL47eGFP (green) and
951 Hoechst 33342 for DNA (blue). Bar, 20µm. (C) Two cell populations (live/green; dead/green)
952 were sorted by flow cytometry after 48 h in hypoxia and normoxia. Cells were labeled with
953 an antibody directed against the VP22 lytic protein and observed by fluorescence
954 microscopy. The VP22 signal (Red) was clearly visible in some live green cells, but never in
955 dead green cells. Bar, 20µm. (D) Kinetic of viral reactivation upon cultivation in hypoxia.
956 3867K were cultivated in normoxia (Nx, dashes grey line) and hypoxia (Hx, plain black line)
957 for 96 h and the viral reactivation measured every 24 h based on UL47eGFP signal by flow
958 cytometry. The % of GFP-positive cells was calculated among live cells. The graph is the
959 result of two independent experiments, with each dot of the curve being the median. (E) The
960 MDV genome copy number upon hypoxia cultivation. 3867K were cultivated in normoxia
961 (Nx, dashes grey line) and hypoxia (Hx, plain black line) for 96 h and the genome copy

number per million cells was measured every 24 h by absolute qPCR. The graph is the result of two independent experiments, with each dot of the curve corresponding to the median.

Figure 2. **MDV lytic genes expression is upregulated during hypoxia.** (A) Schematic diagram of RB-1B genome (Genbank #EF523390) with 16 selected lytic genes. The number of putative HREs identified in the promoter region is given in brackets after each gene name. (B) Heat map showing the differential genes expression of 16 lytic genes as well a *meq* oncogene upon cultivation in hypoxia relatively to normoxia over 72 h. The gene expression was quantified every 24 h and the results are given in fold-changes (scale with colors on the right). This heat-map is representative of two independent experiments.

Figure 3. Hypoxia induces MDV reactivation in MSB-1, a T-cell line latently infected with the BC-1 strain. (A) Viral reactivation assessed by genome copy number measurement. MSB-1 cells were cultivated in normoxia (Nx, dashes grey line) and hypoxia (Hx, plain black line) for 96 h and the genome copy number per million cells was measured every 24 h by absolute qPCR. (B) Images of MSB-1 cultivated in normoxia and hypoxia for 24 and 48 h observed by fluorescence microscopy. The cells were stained with an antibody recognizing the VP22 lytic protein (red) and with Hoechst 33342 for nuclei (blue). Bar, 20 µm. The % of reactivation determined by counting the VP22-positive cells relatively to the cells harboring a non-fragmented nucleus (given as n) is shown on each picture. (C) Heat map showing the differential genes expression of 16 lytic genes as well a *meq* oncogene upon MSB-1 cultivation in hypoxia relatively to normoxia at three time points (24, 48 and 72 h). The results are given in fold-changes (scale with colors on the right).

Figure 4. Hypoxia induces MDV reactivation in a subset of HIF-1α-positive cells. 3867K (A) and MSB-1 (B) were cultivated in normoxia and hypoxia for 48 h. After fixation, "live cells" (eFluor780-negative) were cell-sorted by flow cytometry, stained with an antibody recognizing HIF-1α (in red) and Hoechst 33342 for DNA (blue). (A) For 3867K, reactivation was detected directly with UL47eGFP (green). (B) For MSB-1, reactivation was detected after staining with an antibody against the lytic VP22 protein (green). For each cell line, single channel and overlay images are shown. Bar, 20µm. 3867K and MSB-1 showed a low HIF-1α signal in hypoxia and not in normoxia. A small subset of HIF-1α-positive cells were in reactivation. The fluorescence intensity of HIF-1α per cell was quantified in normoxia and hypoxia in 3867K (C) and MSB-1 (D) cells.

Figure 5. Hypoxia enhances expression of HIF-1-responsive cellular genes in MDV latently infected-T cells. 3867K (A) and MSB-1 (B) cells were cultivated in normoxia or in hypoxia for 72 or 96 h. The mRNA levels of three HIF-1 regulated cellular genes were quantified by RT-qPCR every 24 h and normalized to the RPS-17 gene. mRNA levels are expressed as fold-change in hypoxia relative to normoxia, from one (MSB-1) or two (3867K) independent experiments. The dots correspond to the fold-change of two independent samples, with three technical qPCR repeats each. The median is shown as a long horizontal bar.

Figure 6. HIF1α stabilizers induce MDV reactivation in normoxia in MDV latently infected-T cells. 3867K cultivated in normoxia were treated with different concentrations of CoCl2 or MLN4924 for 24 h. A. Percentage of reactivation (GFP-positive cells) measured on live cells on two independent experiments. After each treatment, cells were stained with the fixable viability dye eFluor780 and analyzed by flow cytometry, for GFP and eFluor780 fluorescence.

1010 The fold changes were calculated relatively to mock-treated cells (Ctrl) (water for CoCl2 and
1011 DMSO for MLN4924). A positive reactivation control was performed with 0.5mM sodium
1012 butyrate (NaBu) for 48 h (n=3 for each condition). B. Expression of HIF-1α and MDV antigens
1013 in 3867K treated with 1µM MLN4924 for 24 h observed by fluorescent microscopy. After
1014 treatment, cells were fixed, centrifuged at low speed on coverslips and stained with
1015 VP22/ICP4 antibodies cocktail (green), HIF-1α antibody (red) and Hoechst 33342 for DNA
1016 (blue). Bar, 20µm. C. The mRNA levels of four viral lytic genes and two HIF-1 regulated
1017 cellular genes were quantified by RT-qPCR after 1µM MLN4924 treatment for 24 h. mRNA
1018 levels are expressed as fold-change relative to RPS-17, from two independent experiments
1019 (with technical triplicates). Each dot corresponds to a single measure. The median is shown
1020 as a long horizontal bar.
1021
1022 **Figure 7. Human HIF-1α is functional in chicken T-cells**. hHIF-1α activity was monitored with
1023 a transactivation assay in normoxia. MSB-1 were transiently co-transfected with pHRE-
1024 d2EGFP reporter plasmid with or without a pCDNA vector expressing HIF-1α, either the
1025 stabilized mutant (P402A/P564A/N803A) (A) or the WT (B). The % of GFP cells was
1026 enumerated by fluorescence microscopy. At least 900 cells were counted in each condition.
1027 For each condition, an image of the cells at 24 h post-transfection is shown. The difference in
1028 GFP-positive cells proportion was significant at each time post-transfection, for both HIF-1
1029 (WT and mutant) (p-value <0.0001, ***; Chi2 test). Bar, 20µm.
1030
1031 **Figure 8. HIF-1α overexpression induces MDV reactivation in MSB-1 in normoxia.** MSB-1
1032 were transfected with the pCDNA vector expressing hHIF-1α mutant or WT, an empty
1033 pCDNA vector or mock-transfected. At 24 h post-transfection, the cells were fixed,

centrifuged at low speed on coverslips, and stained with MDV antigens (VP22/ICP4) antibodies cocktail (green), HIF-1α antibody (red) and Hoechst 33342 for DNA (blue). (A) The percentage of HIF-1α-positive cells in each condition. The difference in HIF-1α-positive cells proportion was significant between WT and mutant and between mutant and pcDNA3 control (adjusted p-value <0.0001, ***; Fisher exact test with a Holm correction for multiple comparison). (B) The percentage of reactivated cells based on MDV antigens-positive cells in each condition. The difference in EGFP-positive cells proportion was significant when HIF-1α (WT or mutant) was present vs pcDNA3 (adjusted p-value <0.0001, ***; Fisher exact test with a Holm correction for multiple comparison). (C) The percentage of HIF-1α-positive cells which were also MDV antigens-positive (reactivated) in each condition. The differences were not significant (adjusted p-value >0.05; Fisher exact test with a Holm correction for multiple comparison) (D). Images of MSB-1 transfected with HIF-1α mut or WT, which were reactivated and HIF-1α positive (green and red; left panel) as well as reactivated and HIF-1α negative (green only; right panel). Bar, 20μm.

Figure 9. HIF-1*α* over-expression activates MDV UL39 and UL49 promoters. A. The expression of hHIF-1α was validated in ESCDL-1, after transient transfection with the hHIFα mut expression vector. The hHIF-1α (red) was detected by fluorescence microscopy as previously. Two cells showed a strong nuclear expression. B. ESCDL-1 cells were co-transfected with a MDV promoter cloned in 5' of a destabilized fLuc gene in pGL4 vector, a TK renilla luciferase (RL) vector for transfection efficacy normalization, with or without the hHIFα mut expression vector. The promoters from seven MDV genes were tested, 5 with HRE (ICP4, ICP27, UL39, UL41 and UL49) and 2 without HRE (UL36, UL45). An empty pGL4 was also assayed as control. Twenty-four hours post-transfection the fluc and RL activities

were measured and the fLuc activity normalized with the RL activity. Each circle represents independent transfection, with hHIF-1α (black circle) or without hHIF-1α (white circle). The horizontal bars represent the median of the quintuplicate. This experiment is representative of at least 2 independent experiments. The differences were significant between with and without hHIFα mut (Mann-Whitney test, p-value <0.01, **). UL39 and UL49 promoters had a strong relative luciferase activity in presence of hHIFα mut, compared to the other promoters tested (with or without HRE).

Figure 10. **Apoptosis mediated by caspase 3 in hypoxia is not promoting MDV reactivation.** A. 3867K cultivated in normoxia were treated or not with 50µM of Z-DEVD-FMK for 24 h, and the caspase 3/7 activity was next measured with the luminescent Caspase 3/7-Glo® assay. The difference was significant between cells treated and non-treated with Z-DEVD-FMK (Mann-Whitney test, p-value =0.0022, **). B. 3867K were cultivated in hypoxia with or without 50µM of Z-DEVD-FMK. The caspase 3/7 activity (black dots, replicates from two independent experiments) was measured at 48 h and 72 h. At both timepoints, the differences were significant (Mann-Whitney test, p-value <0.01, **). In parallel, the percentage of reactivated cells among live cells (green squares) from two independent experiments was measured based on UL47eGFP signal and cell mortality quantified by flow cytometry.

Table 1. Percentage of dead cells in 3867K and MSB-1 during hypoxia or normoxia cultivation

	24 h		48 h		7 2h		96 h	
	Normoxia	**Hypoxia**	**Normoxia**	**Hypoxia**	**Normoxia**	**Hypoxia**	**Normoxia**	**Hypoxia**
3867K Expt#1	20.63	32.35	13.15	44.11	12.52	51.79	14.35	52.36
Expt#2	21.93	39.92	19.00	48.66	20.99	59.34	25.22	66.42
MSB-1	25.85	57.96	28.80	79.22	34.10	85.07	44.31	85.61

1085 **Table 2**. Viral and cellular primers used in this study for RT-qPCR

Gene name	**Forward primer sequence** (5' to 3')	**Reverse primer sequence** (5' to 3')	**NCBI Reference sequence**
MDV			EF523390
ICP4	TTTCTAGCAAGGAGCGACGC	CGTACTTGCGCTTACGGGAA	
ICP27	CTCGCGAGTCCGATGACATG	GTTCCTGCGTACACGGTGGC	
UL39	ACGGGGGTAGCAAATTGGAG	CAGCTCGCAGTAGAGGTTCC	
UL42	TTAGCGACGACGGACTGATG	CCCGCGCCATTCATATTCAC	
UL30	CTGTTGGGGACACTATGCGT	CCGATTCCGCTTCGTATCGT	
UL41	CCCGGGGTGTTTCCTCTTAC	TTCTGGGCGACTACATGCAC	
pp38	TTGCATTCTCTGACTCCACGG	GCTGGCCGAAAGACAAAACC	
UL31	GCTCTGTCGTTTCGTCCCAA	GAGGCGGTTGCGGATAACT	
UL34	CGATGAAACGCACAGAAGTGG	ATCGTCGTCACACATTCGCC	
UL13	GGGATTAGGACCCTCGGTGA	TCTCGGCAAAGCAGTTGTGT	
UL47	GTATCACTACCGCGACGACC	CGATACGCTAGAGGAGAGCG	
UL48	CAGGAGCAGTCAAAACACGC	CTTTCTACCACGCGGGATGT	
UL49-VP22	TGCTCGCAGACCATCAACAC	GAAACGTCTTCCGATACGGC	
UL27-gB	GTCCGATAGAACGGCGGTAG	TGAGTTGCATGGCGAGGAAT	
UL44-gC	GCCGCATTCCAGTATGGGAC	CTTCATCGAAGGGGTAGCC	
US7-gI	CCTCTTTCGAGGCATCTGGT	AATCCGCAGAACGCAACAAG	
meq	GTCCCCCTCGATCTTTCTC	CGTCTGCTTCCTGCGTCTTC	
Gallus gallus			
GLUT1	GAGAGCGGCAGCAAGATGAC	CTTCTGCGGGCGATTGATGA	NM_205209
LDHA	TTAACTTGGCCAACGCAACGTCAAT	TCCACTGGGTTTGAGACAATCAG	NM_205284
iNOS	TACTGCGTGTCCTTTCAACG	CCCATTCTTCTTCCAACCTC	NM_204961
RPS17	ACACCCGTCTGGGCAACGAC	CCCGCTGGATGCGCTTCATC	NM_204217

1086

1087

Table 3. Primers used in this study for MDV promoters cloning

Gene name	Primer sequence (5′ to 3′)*	Amplicon length (bp)
UL39XhoI	GTC**CTCGAG**CTTCATCATCTCTATACCTTGTG	712
UL39HindIII	CTG**AAGCTT**AGCAGATTTTTAGTCGCAGAGTG	
UL41XhoI	CTG**CTCGAG**ATAATTGCAATGCGCATGTTCTA	512
UL41HindIII	CTG**AAGCTT**GATGACCCTCGCAGTTTTTAAATAT	
UL49XhoI	CTG**CTCGAG**ATTGCAGACGCCAGGGAACTGTT	512
UL49HindIII	CTG**AAGCTT**GATAACTAAGATATAATATTAAA	
ICP4XhoI	CTG**CTCGAG**CCTGATACCGCACTTTG	452
ICP4HindIII	CTG**AAGCTT**AATCCCCACGTCTTCGTCAAAAGC	
ICP27XhoI	CTG**CTCGAG**CTATCGATGTATTTTGTACCATG	536
ICP27HindIII	CTG**AAGCTT**GCGAGAGAATGCATCTACAGACA	
UL36XhoI	CTG**CTCGAG**CGGTGAAATAGAATTTGCCG	512
UL36HindIII	CTG**AAGCTT**TTTACACTCAATTTATATGA	
UL45XhoI	CTG**CTCGAG**TTTGTCATGGAGATATCGTC	512
UL45HindIII	CTG**AAGCTT**TCTTATACGATCATGTCTAT	

* restriction sites in bold

Figure 1

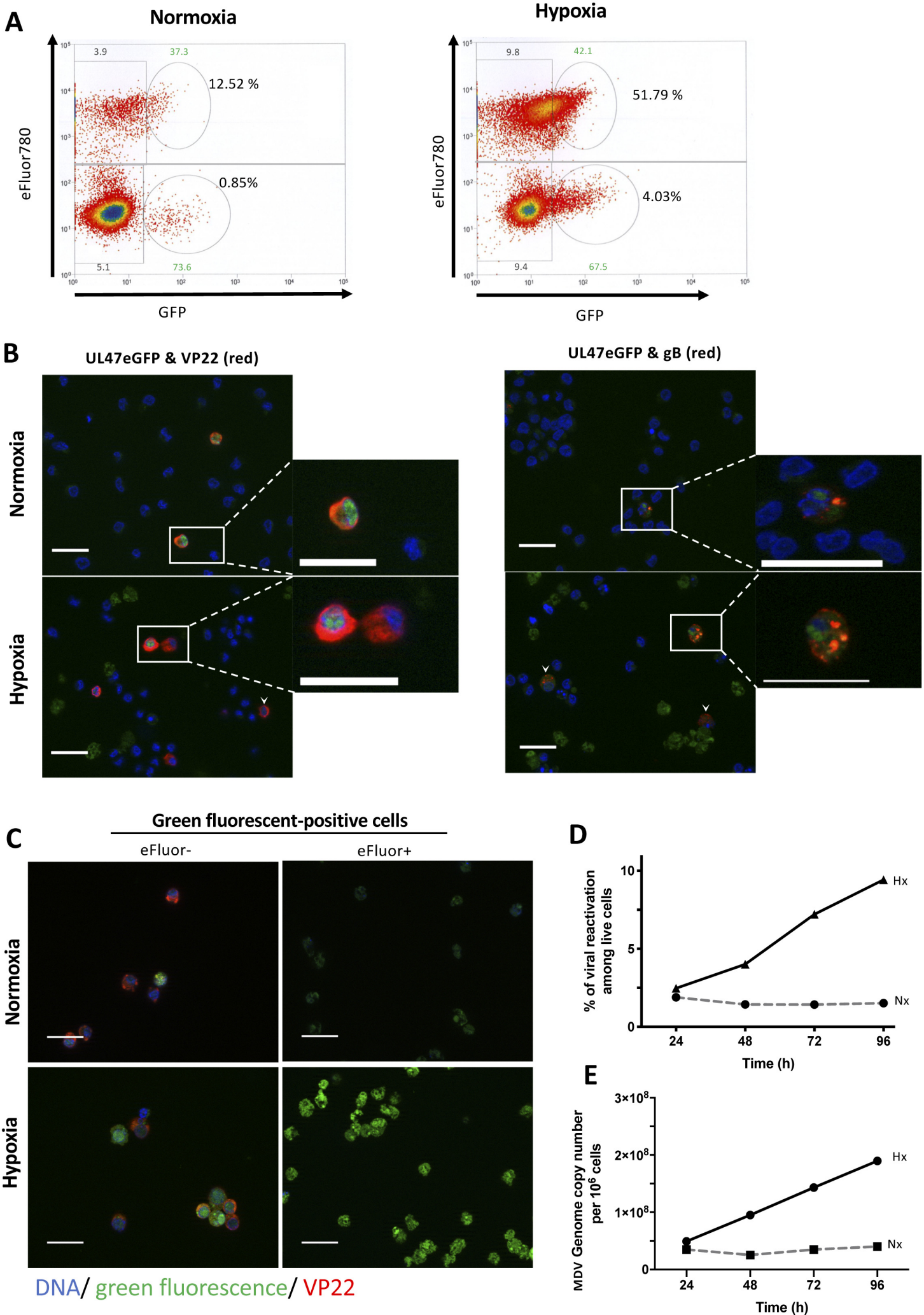
A
Normoxia
Hypoxia
eFluor780
GFP
3.9
37.3
12.52 %
0.85%
5.1
73.6
9.8
42.1
51.79 %
4.03%
9.4
67.5
B
UL47eGFP & VP22 (red)
UL47eGFP & gB (red)
Normoxia
Hypoxia
C
Green fluorescent-positive cells
eFluor-
eFluor+
Normoxia
Hypoxia
DNA/ green fluorescence/ VP22
D
% of viral reactivation among live cells
Hx
Nx
Time (h)
E
MDV Genome copy number per 10^6 cells
Hx
Nx
Time (h)

Figure 2

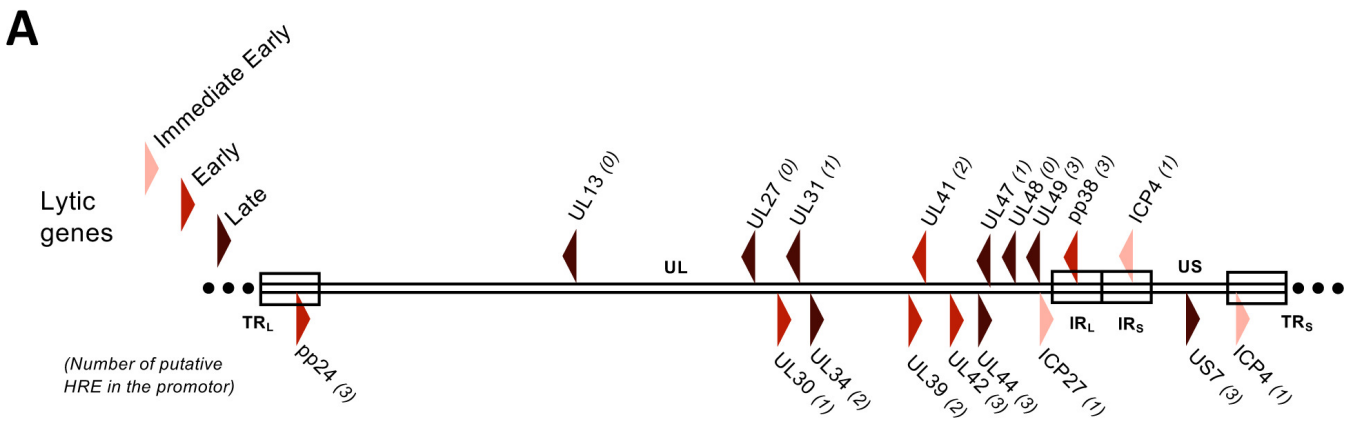
A
Immediate Early
Early
Late
Lytic genes
(Number of putative HRE in the promotor)
TRL
IRL
IRS
TRS
UL
US
UL13 (0)
UL27 (0)
UL31 (1)
UL41 (2)
UL47 (1)
UL48 (0)
UL49 (3)
pp38 (3)
ICP4 (1)
pp24 (3)
UL30 (1)
UL34 (2)
UL39 (2)
UL42 (3)
UL44 (3)
ICP27 (1)
US7 (3)
ICP4 (1)

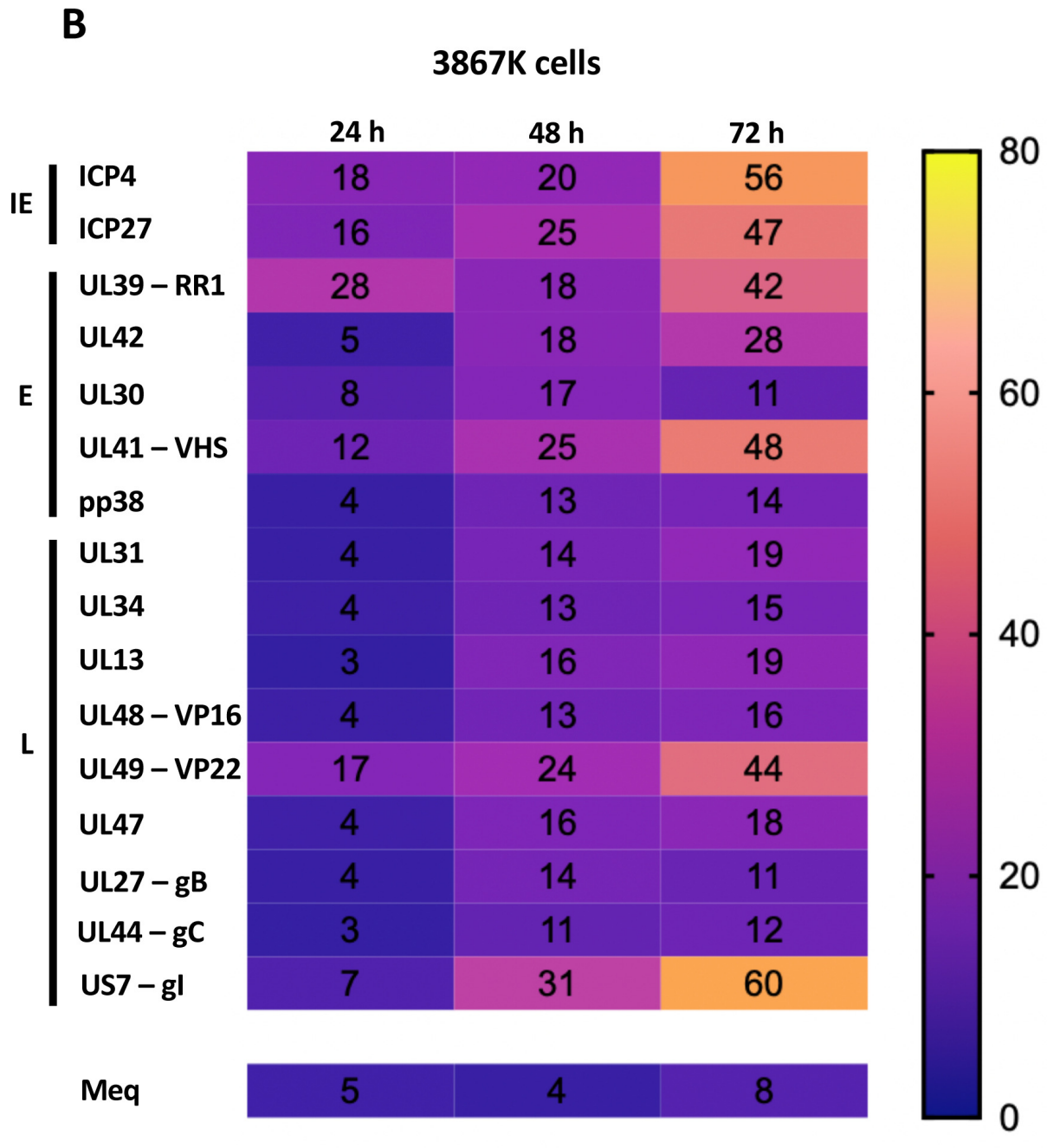
B
3867K cells
24 h
48 h
72 h
IE
ICP4 18 20 56
ICP27 16 25 47
E
UL39 – RR1 28 18 42
UL42 5 18 28
UL30 8 17 11
UL41 – VHS 12 25 48
pp38 4 13 14
L
UL31 4 14 19
UL34 4 13 15
UL13 3 16 19
UL48 – VP16 4 13 16
UL49 – VP22 17 24 44
UL47 4 16 18
UL27 – gB 4 14 11
UL44 – gC 3 11 12
US7 – gI 7 31 60
Meq 5 4 8
80
60
40
20
0

Figure 3

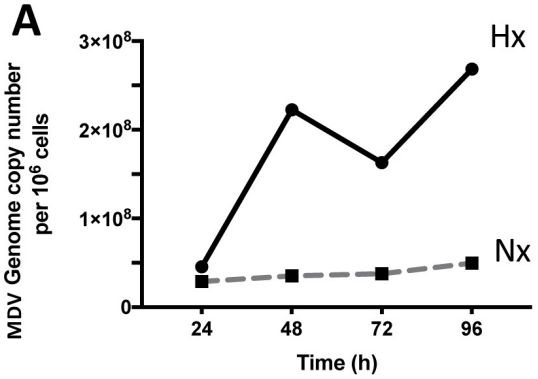
A
MDV Genome copy number per 10^6 cells
3×10^8
2×10^8
1×10^8
0
24
48
72
96
Time (h)
Hx
Nx

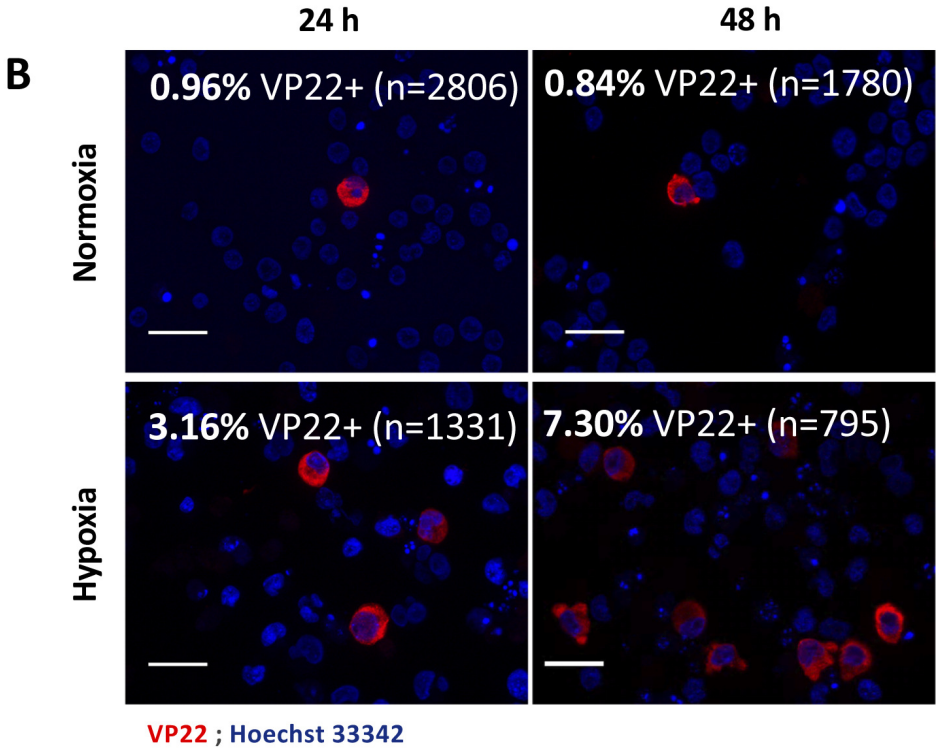
B
24 h
48 h
Normoxia
Hypoxia
0.96% VP22+ (n=2806)
0.84% VP22+ (n=1780)
3.16% VP22+ (n=1331)
7.30% VP22+ (n=795)
VP22 ; Hoechst 33342

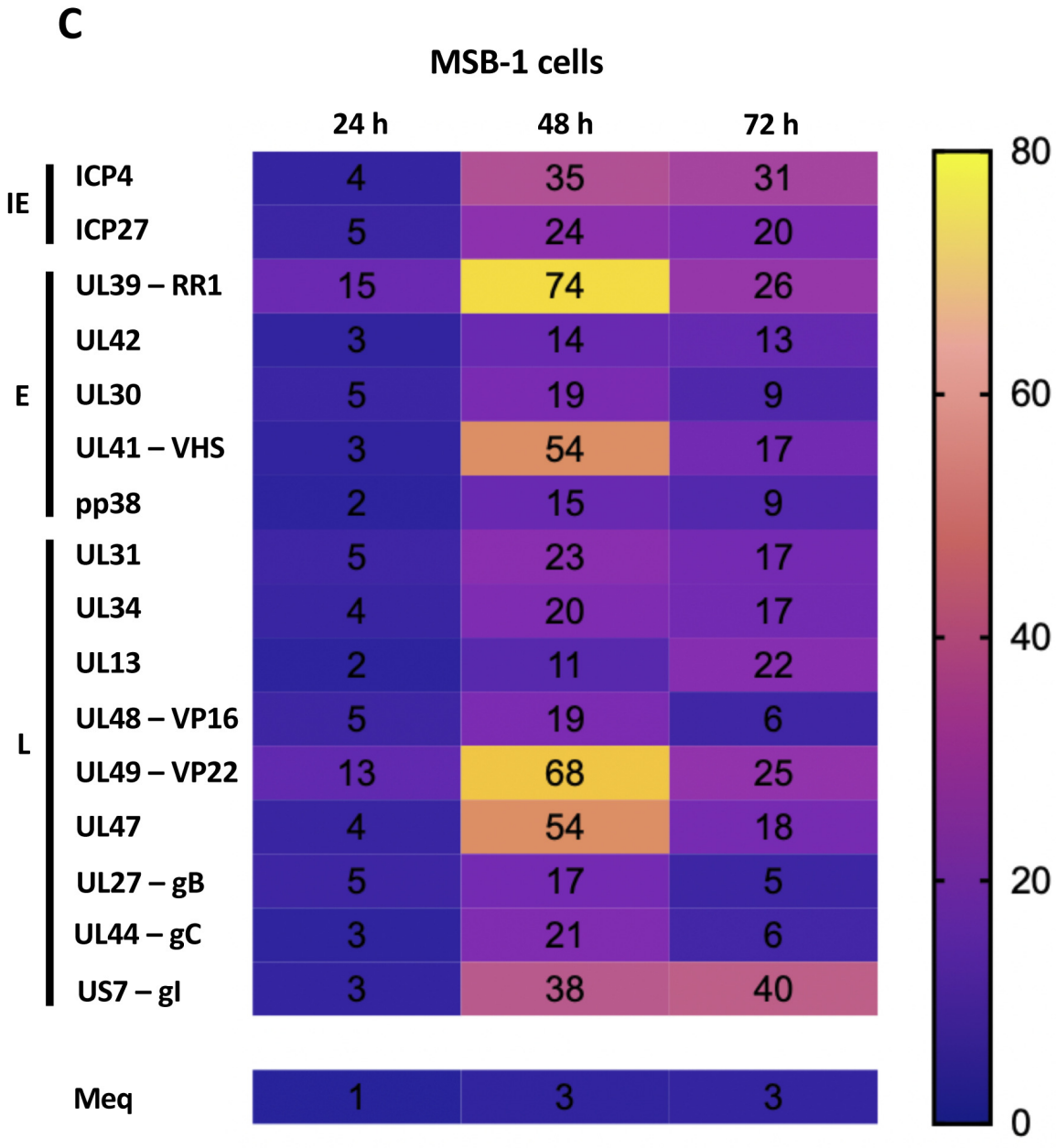
C
MSB-1 cells
24 h
48 h
72 h
IE
ICP4 4 35 31
ICP27 5 24 20
E
UL39 – RR1 15 74 26
UL42 3 14 13
UL30 5 19 9
UL41 – VHS 3 54 17
pp38 2 15 9
L
UL31 5 23 17
UL34 4 20 17
UL13 2 11 22
UL48 – VP16 5 19 6
UL49 – VP22 13 68 25
UL47 4 54 18
UL27 – gB 5 17 5
UL44 – gC 3 21 6
US7 – gI 3 38 40
Meq 1 3 3
80
60
40
20
0

Figure 4

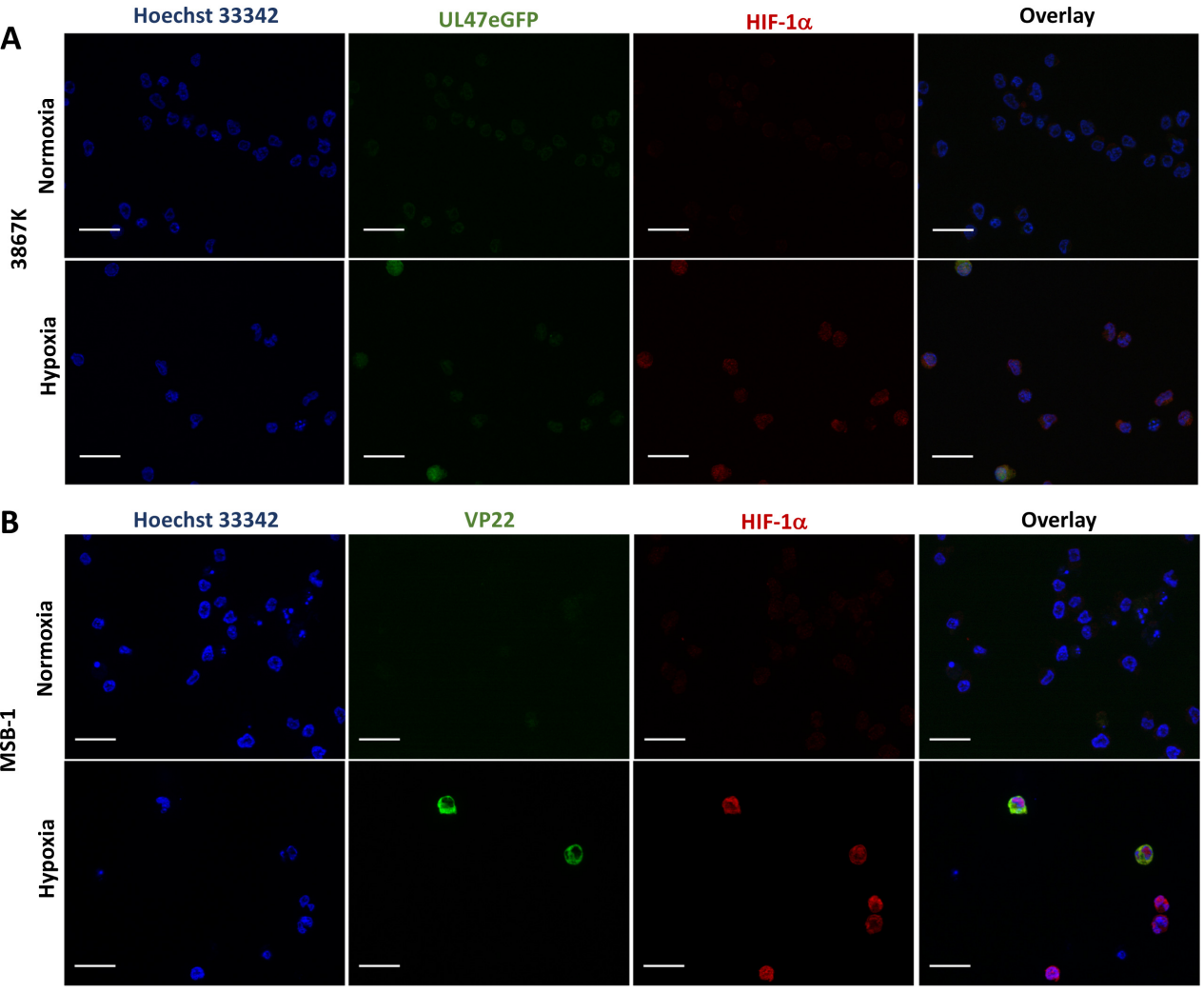
A
Hoechst 33342
UL47eGFP
HIF-1α
Overlay
3867K
Normoxia
Hypoxia
B
Hoechst 33342
VP22
HIF-1α
Overlay
MSB-1
Normoxia
Hypoxia

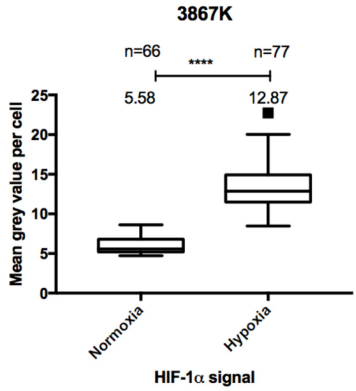
C
3867K
n=66
n=77
****
5.58
12.87
Mean grey value per cell
0
5
10
15
20
25
Normoxia
Hypoxia
HIF-1α signal

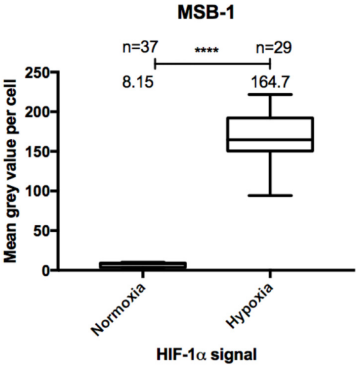
D
MSB-1
n=37
n=29
****
8.15
164.7
Mean grey value per cell
0
50
100
150
200
250
Normoxia
Hypoxia
HIF-1α signal

Figure 5

A 3867K

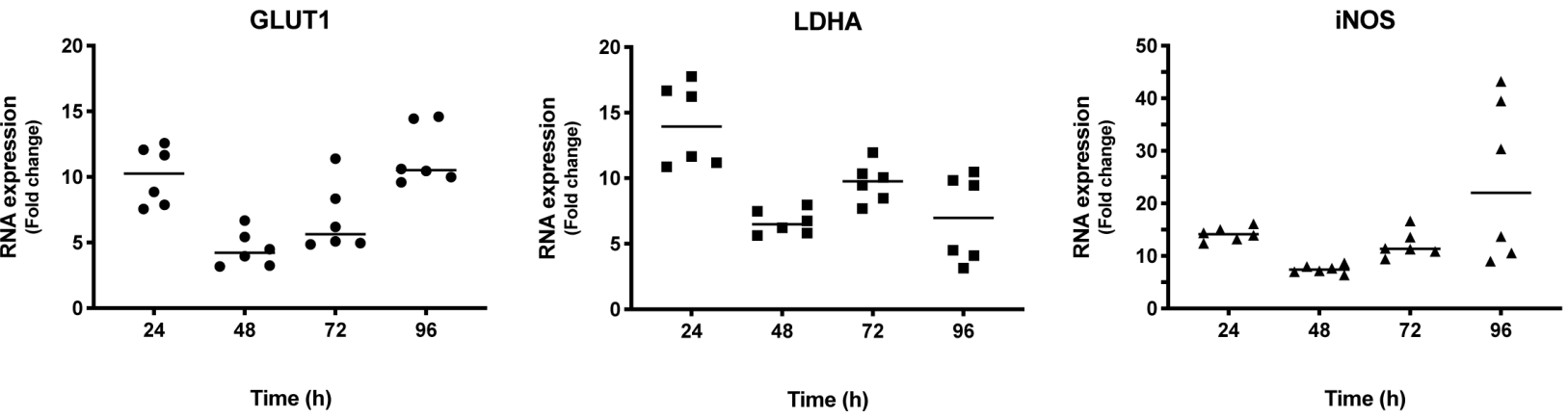

B MSB-1

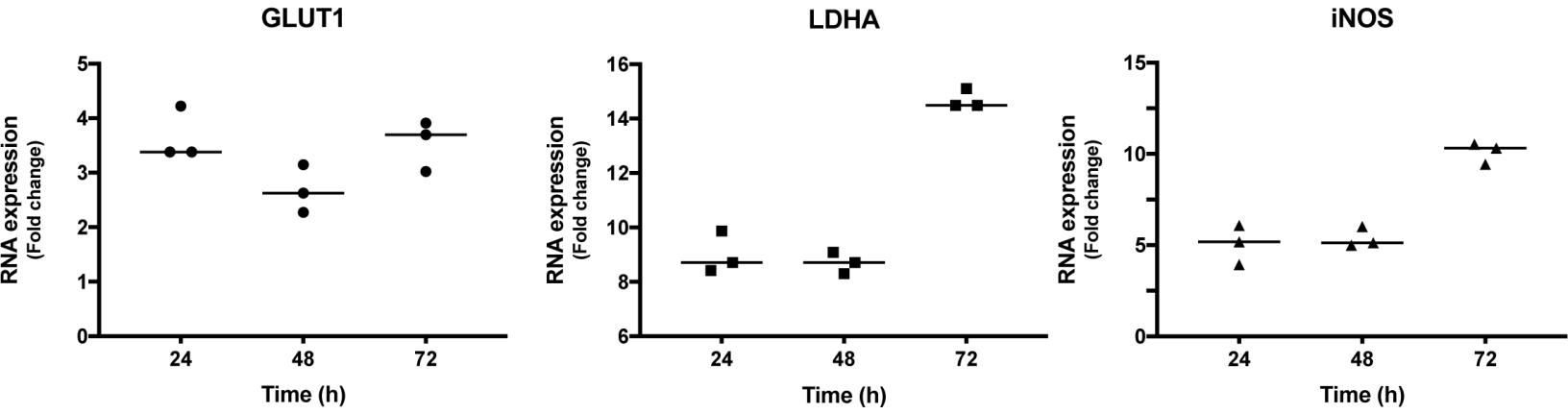

Figure 6

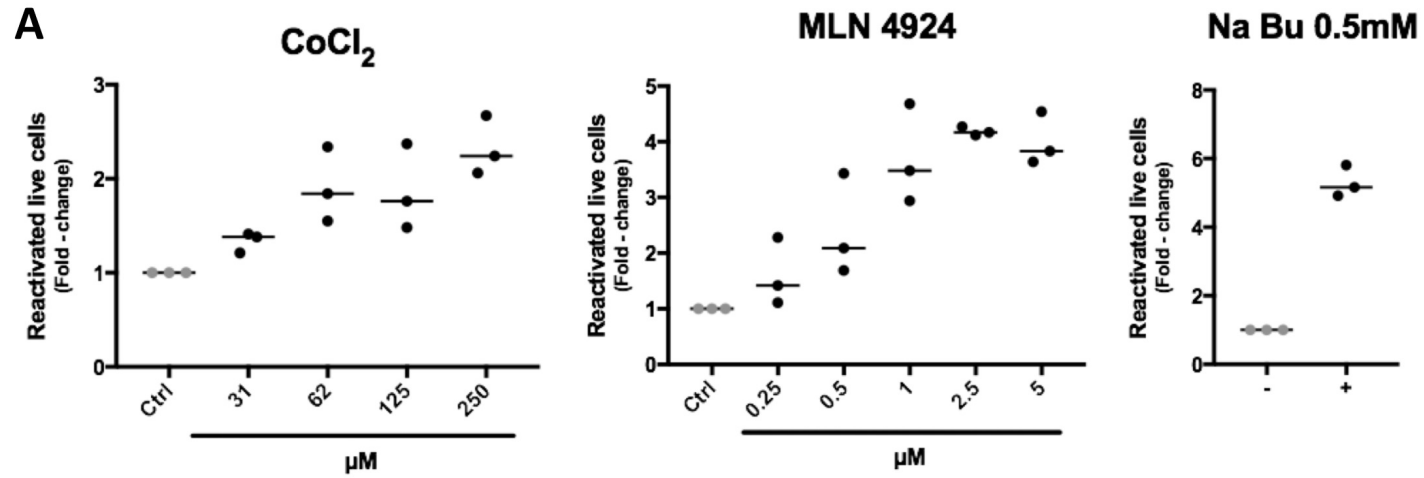
A
CoCl2
MLN 4924
Na Bu 0.5mM
Reactivated live cells
(Fold - change)
Ctrl
31
62
125
250
μM
0.25
0.5
1
2.5
5
-
+

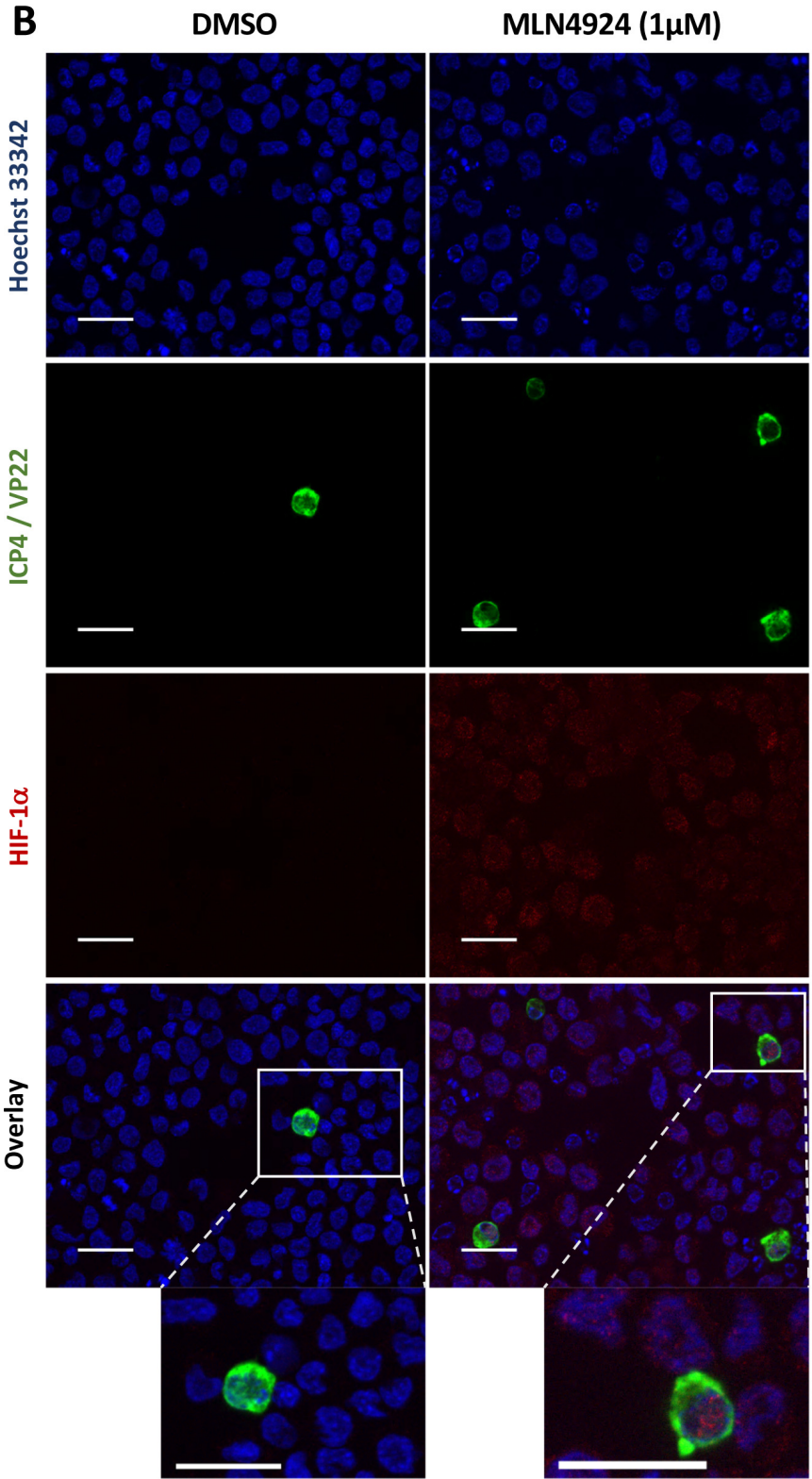
B
DMSO
MLN4924 (1μM)
Hoechst 33342
ICP4 / VP22
HIF-1α
Overlay

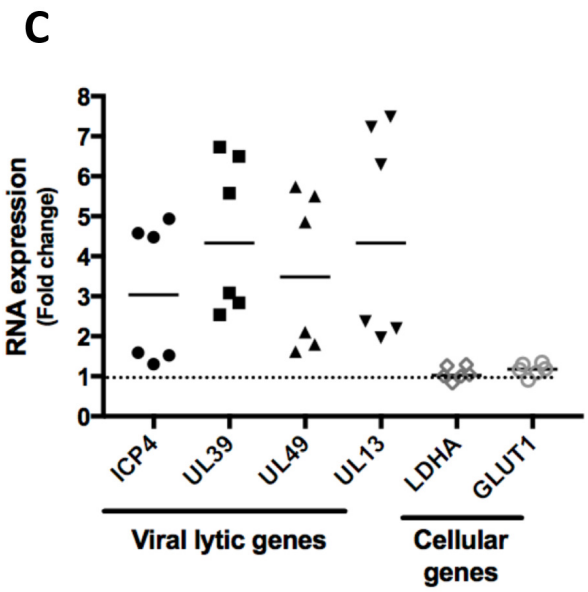
C
RNA expression
(Fold change)
ICP4
UL39
UL49
UL13
LDHA
GLUT1
Viral lytic genes
Cellular genes

Figure 7

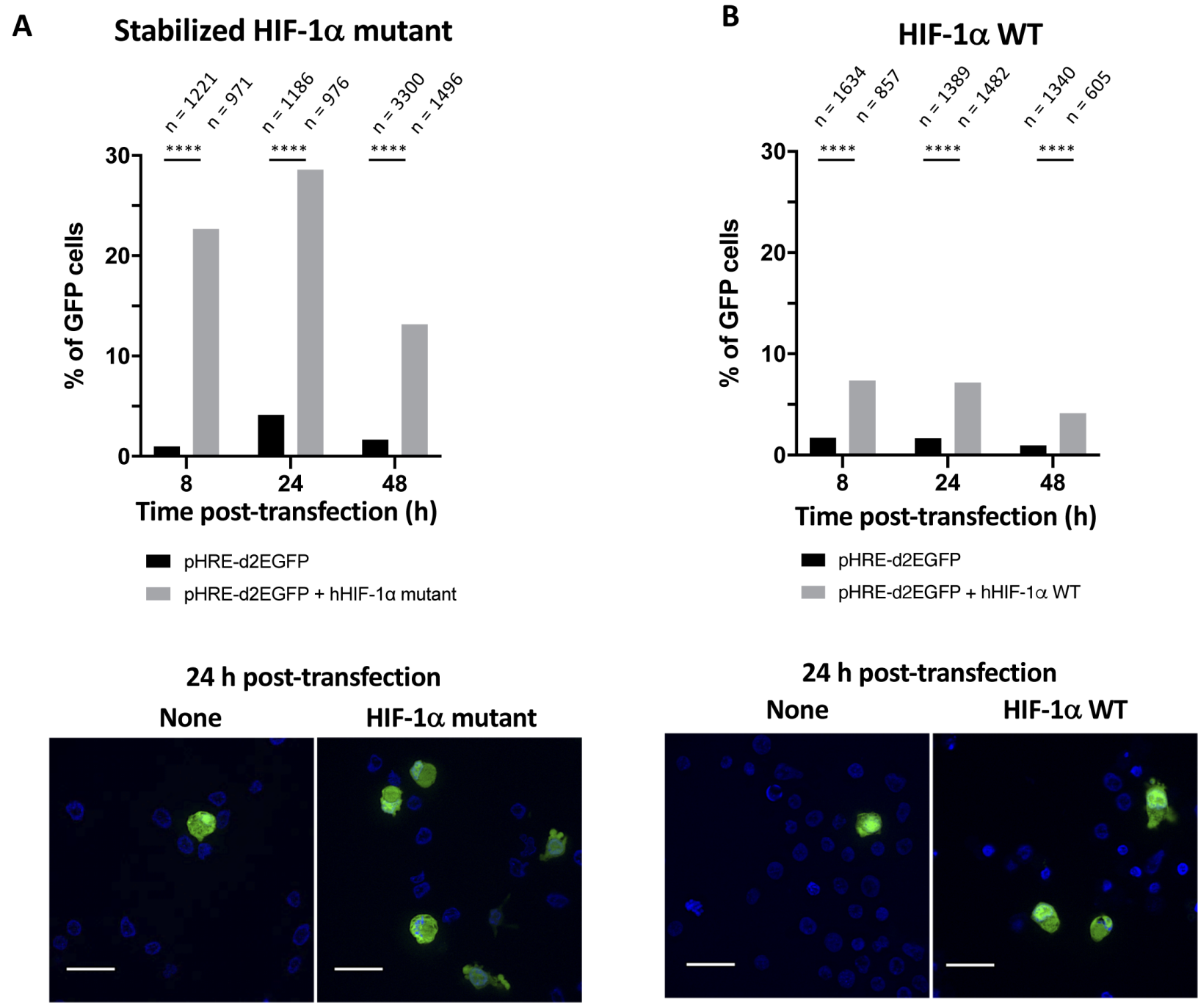
A
Stabilized HIF-1α mutant
n = 1221
n = 971
n = 1186
n = 976
n = 3300
n = 1496
****
****
****
30
20
10
0
% of GFP cells
8
24
48
Time post-transfection (h)
pHRE-d2EGFP
pHRE-d2EGFP + hHIF-1α mutant
B
HIF-1α WT
n = 1634
n = 857
n = 1389
n = 1482
n = 1340
n = 605
****
****
****
30
20
10
0
% of GFP cells
8
24
48
Time post-transfection (h)
pHRE-d2EGFP
pHRE-d2EGFP + hHIF-1α WT
24 h post-transfection
None
HIF-1α mutant
24 h post-transfection
None
HIF-1α WT

Figure 8

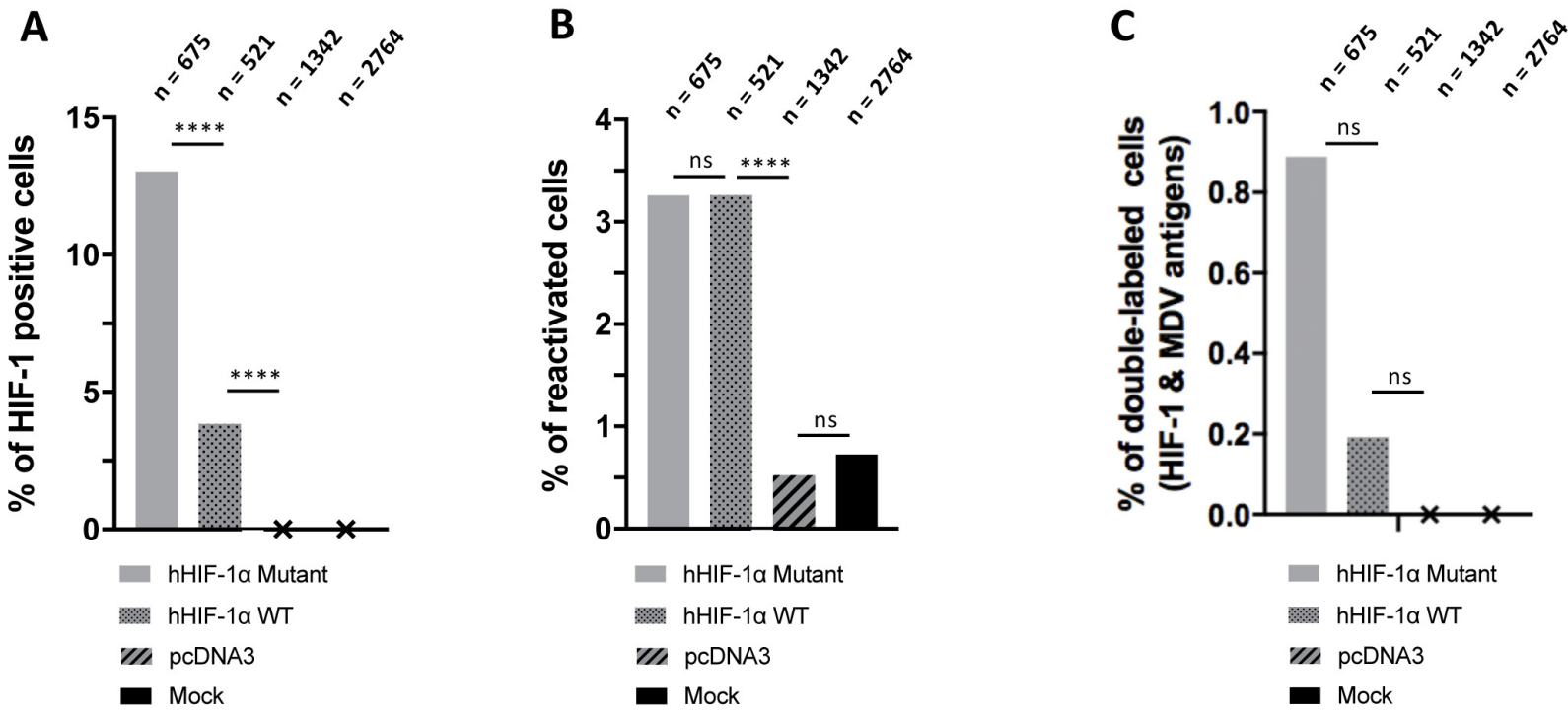
A
n = 675
n = 521
n = 1342
n = 2764
****
****
% of HIF-1 positive cells
15
10
5
0
hHIF-1α Mutant
hHIF-1α WT
pcDNA3
Mock
B
n = 675
n = 521
n = 1342
n = 2764
ns
****
ns
% of reactivated cells
4
3
2
1
0
hHIF-1α Mutant
hHIF-1α WT
pcDNA3
Mock
C
n = 675
n = 521
n = 1342
n = 2764
ns
ns
% of double-labeled cells (HIF-1 & MDV antigens)
1.0
0.8
0.6
0.4
0.2
0.0
hHIF-1α Mutant
hHIF-1α WT
pcDNA3
Mock

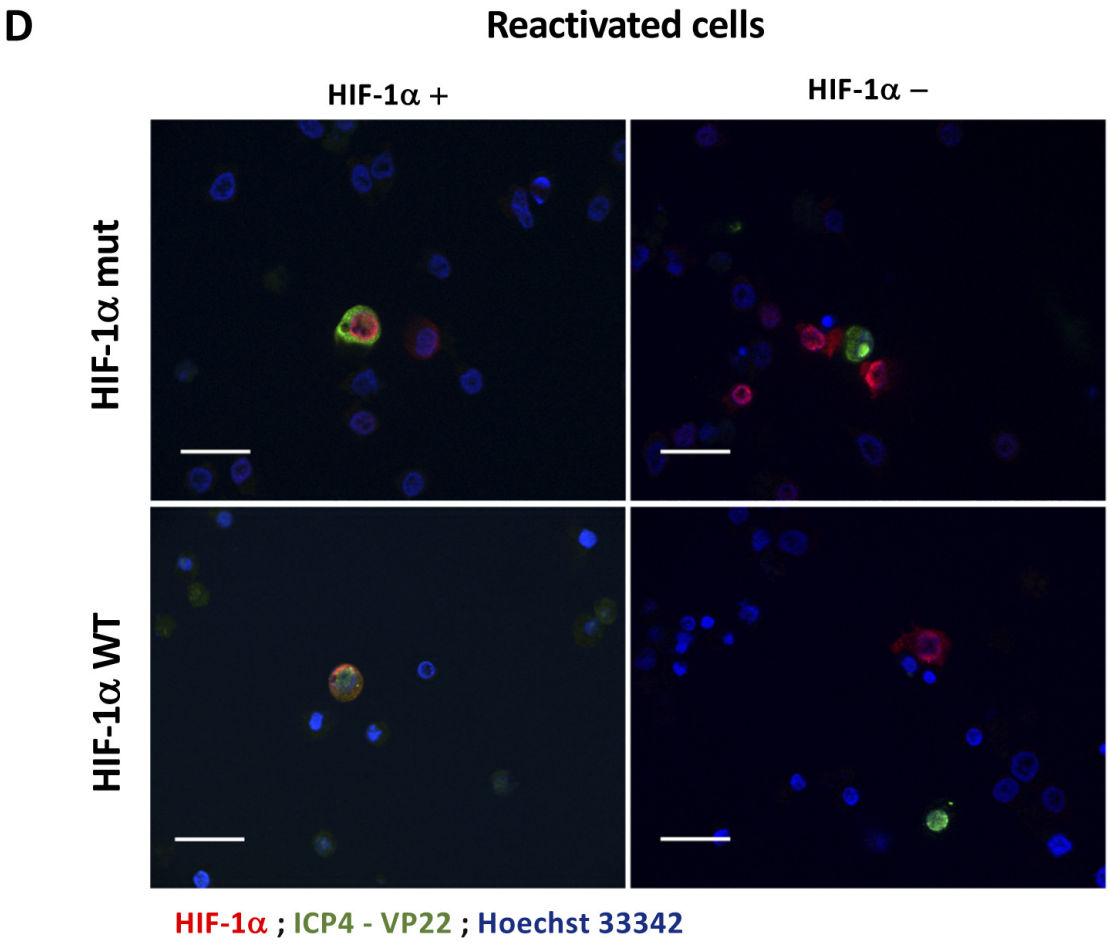
D
Reactivated cells
HIF-1α +
HIF-1α –
HIF-1α mut
HIF-1α WT
HIF-1α ; ICP4 - VP22 ; Hoechst 33342

Figure 9

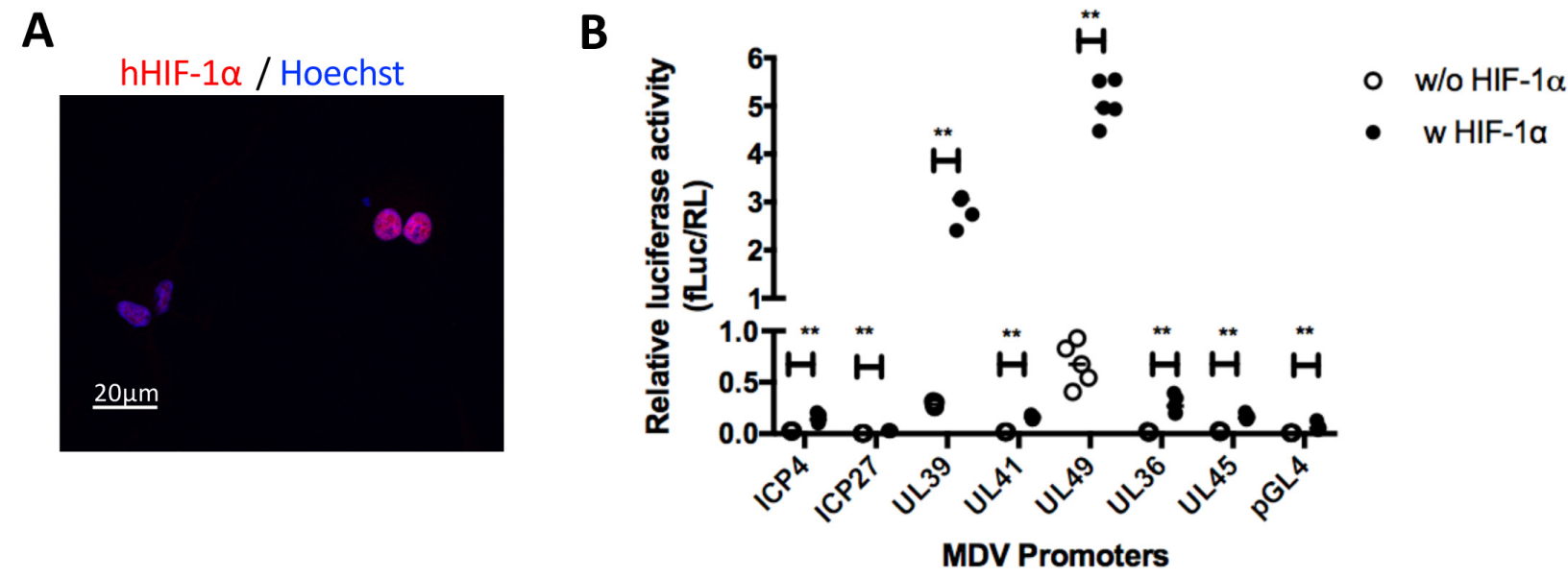
A
hHIF-1α / Hoechst
20μm
B
Relative luciferase activity (fLuc/RL)
6
5
4
3
2
1
1.0
0.5
0.0
**
ICP4
ICP27
UL39
UL41
UL49
UL36
UL45
pGL4
MDV Promoters
w/o HIF-1α
w HIF-1α

Figure 10

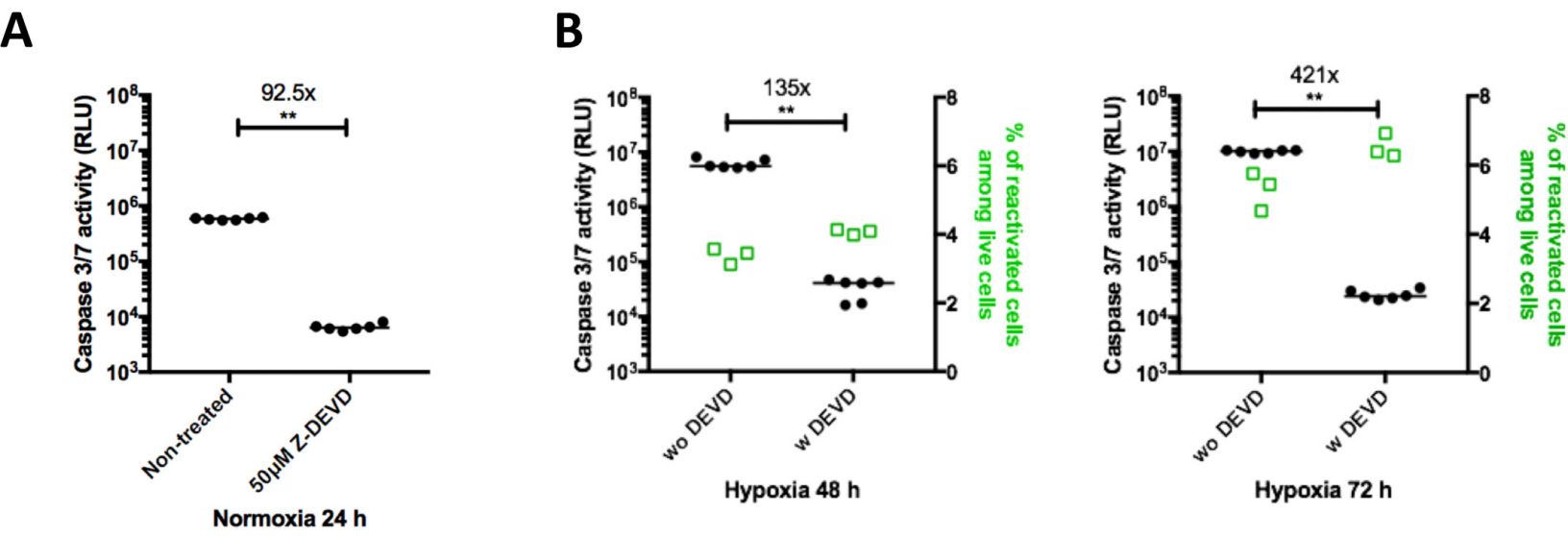
A
B
92.5x
**
Caspase 3/7 activity (RLU)
Non-treated
50μM Z-DEVD
Normoxia 24 h
135x
**
% of reactivated cells among live cells
wo DEVD
w DEVD
Hypoxia 48 h
421x
**
Hypoxia 72 h